Triple isotope (δD, δ^{17}O, δ^{18}O) study on precipitation, drip water and speleothem fluid inclusions for a Western Central European cave (NW Switzerland)

Stéphane Affolter [a, c, *], Anamaria D. Häuselmann [b, c], Dominik Fleitmann [d, c], Philipp Häuselmann [e], Markus Leuenberger [a, c]

[a] Climate and Environmental Physics, Physics Institute, University of Bern, 3012 Bern, Switzerland
[b] Institute of Geological Sciences, University of Bern, 3012 Bern, Switzerland
[c] Oeschger Centre for Climate Change Research, University of Bern, 3012 Bern, Switzerland
[d] Department of Archaeology, School of Archaeology, Geography and Environmental Sciences and Centre for Past Climate Change, University of Reading, Whiteknights, PO Box 227, Reading RG6 6AB, UK
[e] Swiss Institute for Speleology and Karst Studies, 2301 La Chaux-de-Fonds, Switzerland

A R T I C L E   I N F O

A B S T R A C T

Deuterium (δD) and oxygen (δ^{18}O) isotopes are powerful tracers of the hydrological cycle and have been extensively used for paleoclimate reconstructions as they can provide information on past precipitation, temperature and atmospheric circulation. More recently, the use of ^{17}O$_{excess}$ derived from precise measurement of δ^{17}O and δ^{18}O gives new and additional insights in tracing the hydrological cycle whereas uncertainties surround this proxy. However, ^{17}O$_{excess}$ could provide additional information on the atmospheric conditions at the moisture source as well as about fractionations associated with transport and site processes. In this paper we trace water stable isotopes (δD, δ^{17}O and δ^{18}O) along their path from precipitation to cave drip water and finally to speleothem fluid inclusions for Milandre cave in northwestern Switzerland. A two year-long daily resolved precipitation isotope record close to the cave site is compared to collected cave drip water (3 months average resolution) and fluid inclusions of modern and Holocene stalagmites. Amount weighted mean δD, δ^{18}O and δ^{17}O are -71.0‰, -9.9‰, -5.2‰ for precipitation, -60.3‰, -8.7‰, -4.6‰ for cave drip water and -61.3‰, -8.3‰, -4.7‰ for recent fluid inclusions respectively. Second order parameters have also been derived in precipitation and drip water and present similar values with 18 per meg for ^{17}O$_{excess}$ whereas d-excess is 1.5‰ more negative in drip water. Furthermore, the atmospheric signal is shifted towards enriched values in the drip water and fluid inclusions (Δ of ~ + 10‰ for δD). The isotopic composition of cave drip water exhibits a weak seasonal signal which is shifted by around 8−10 months (groundwater residence time) when compared to the precipitation. Moreover, we carried out the first δ^{17}O measurement in speleothem fluid inclusions, as well as the first comparison of the δ^{17}O behaviour from the meteoric water to the fluid inclusions entrapment in speleothems. This study on precipitation, drip water and fluid inclusions will be used as a speleothem proxy calibration for Milandre cave in order to reconstruct paleotemperatures and moisture source variations for Western Central Europe.

© 2015 Elsevier Ltd. All rights reserved.

1. Introduction

Water isotopes in precipitation (hereafter discussed as δD$_p$, δ^{17}O$_p$ and δ^{18}O$_p$) reflect the moist air masses history through moisture source, atmospheric circulation and evaporation/condensation processes. On a regional scale δ^{18}O$_p$ varies according to surface air temperature, amount of precipitation, moisture

source origin and rainout effect (Rozanski et al., 1992; Araguas−Araguas et al., 2000). These changes are recorded in speleothems, which are therefore now widely used for continental paleoclimate reconstructions. However, in order to interpret $\delta^{18}O_p$ in speleothems, an understanding of the key processes that govern the isotopic composition of precipitation, cave drip water, speleothem calcite and fluid inclusions must be well documented. Only with these prerequisites speleothem data can be interpreted in terms of climate and hydrology (Riechelmann et al., 2011). Cave monitoring studies constitute a new standard for the interpretation of speleothem proxies and characterising the relationship between water isotopes of precipitation and cave drip water is becoming routine in caves worldwide (Cruz et al., 2005; Moerman et al., 2010; Cuthbert et al., 2014; Genty et al., 2014).

Stalagmites in particular allow the reconstruction of climate for long time intervals throughout the Quaternary (Cheng et al., 2009; Fleitmann et al., 2009; Meckler et al., 2012). They can be precisely dated using laminae counting (Fleitmann et al., 2004; Shen et al., 2013; Duan et al., 2015) or more commonly by Uranium series dating (Cheng et al., 2013) and can provide information on past climate change at high resolution (Henderson, 2006).

The majority of speleothem-based paleoclimate reconstructions rely on calcite geochemistry (Shakun et al., 2007). Routinely measured are $\delta^{18}O$ and $\delta^{13}C$ for calcite ($\delta^{18}O_c$ hereafter), which are respectively proxies for moisture supply (Burns et al., 2001; Fleitmann et al., 2003; Kennett et al., 2012; Vaks et al., 2013; Luetscher et al., 2015) and vegetation dynamics (Genty et al., 2010; Rudzka et al., 2011; Blyth et al., 2013) above the cave. Although widely used, $\delta^{18}O_c$ can be influenced by several processes above or within the cave such as temperature- and humidity-driven isotope fractionation of the atmospheric water cycle, fractionation associated with the biospheric exchanges, equilibrium and kinetic fractionation in the epikarst and within the cave during calcite precipitation. These effects can make the interpretation of $\delta^{18}O_c$ difficult (Lachniet, 2009).

Fluid inclusions represent past drip water and are consequently relics of past precipitation above the cave at the time when fluid inclusions were sealed (Schwarcz et al., 1976). Hence, they can be used as a direct proxy for paleotemperature or moisture history (Fleitmann et al., 2003; van Breukelen et al., 2008; Griffiths et al., 2010). Based on the correlation between mean annual temperature and mean annual $\delta^{18}O_p$ on a global scale (Dansgaard, 1964), past temperature can thus be reconstructed using for instance the relationship that exists for calcite precipitation at equilibrium (Kim and O'Neil, 1997). However, one has to consider that the seasonal distribution of precipitation is an additional factor that could easily yield misleading temperature estimates for the past. Moreover, most cave stalagmites are not deposited in oxygen equilibrium with their parent drip waters (McDermott et al., 2006). Thus, it was observed that temperatures calculated on modern speleothems using an empirical relationship (Craig, 1965) were closer to corresponding cave air temperatures. Recently, Tremaine et al. (2011) suggested a new empirical calibration based on several caves data already taking into account a mean disequilibrium that seems to provide more reliable speleothem-based temperature estimates. A comparison of multiple proxies (Meckler et al., 2015) shows the potential of speleothems for absolute paleotemperature reconstructions by comparing the results of four different paleo-thermometers that are (i) speleothem fluid inclusions (Dublyansky and Spötl, 2009; Affolter et al., 2014), (ii) liquid−vapour homogenization of fluid inclusions (Krüger et al., 2011), (iii) noble gases concentration in stalagmite water (Vogel et al., 2013), and (iv) clumped isotopes (Meckler et al., 2014). It is thus important to monitor the isotope proxies from the precipitation falling above the cave to evaluate whether the isotopic composition of cave drip and

speleothem fluid inclusion water is comparable. So far, most investigations study the relationship between precipitations and drip water, while in this study we additionally investigate the climate signal transmission to speleothem fluid inclusions. Recent developments in speleothem fluid inclusion measurement techniques allow determining both δD_{fi} and $\delta^{18}O_{fi}$ on a single sample (Arienzo et al., 2013; Affolter et al., 2014). Here we provide a further development of the method by measuring $\delta^{17}O$ in fluid inclusion water ($\delta^{17}O_{fi}$) offering new horizons for paleoclimate research based on speleothems. $\delta^{17}O$ measurements on water samples were so far achieved using CoF_3 fluorination of water (Landais et al., 2012a), but a more recent laser absorption spectroscopy based technique allows now fast and simple triple isotope measurements on water samples (Steig et al., 2014).

The d-excess and $^{17}O_{excess}$ can be calculated from the triple isotope measurements on water aliquots. Deuterium excess is obtained from hydrogen (δD) and oxygen ($\delta^{18}O$) isotopes values and is defined as $d = \delta D - 8 \times \delta^{18}O$ (Dansgaard, 1964). It carries information about the ocean surface conditions and is used to characterise the disequilibrium conditions at the moisture source. The d-excess is mainly dependent on sea surface temperature, normalised relative humidity and wind speed at the moisture source (Jouzel and Merlivat, 1984; Uemura et al., 2008; Pfahl and Sodemann, 2014) but is also dependent on local conditions such as recycling of local moisture. Similarly to d-excess, $^{17}O_{excess}$ is calculated (see section 3.2.2) from small variations in oxygen isotopes ($\delta^{17}O$ and $\delta^{18}O$) and corresponds to the deviation from the line of 0.528 corresponding to meteoric waters (Luz and Barkan, 2010). It constitutes a promising, but debated parameter to provide additional information on the water cycle (Winkler et al., 2012; Schoenemann et al., 2014; Li et al., 2015). The $^{17}O_{excess}$ can be used as an indicator of evaporation conditions at the moisture source (Angert et al., 2004; Barkan and Luz, 2007) and has been so far mostly studied in the Polar Regions (Landais et al., 2008, 2012b; Schoenemann et al., 2014) and poorly in the lower latitudes (Landais et al., 2010; Luz and Barkan, 2010; Li et al., 2015). Over the ocean, $^{17}O_{excess}$ is negatively correlated with the normalised relative humidity (Uemura et al., 2010). A direct link with relative humidity was observed in the coastal area of Antarctica (Winkler et al., 2012) but Schoenemann et al. (2014) showed that in Antarctica, $^{17}O_{excess}$ has a strong dependence on the atmospheric temperature during transport due to the temperature dependence of supersaturation that override any information about the relative humidity. Furthermore, $^{17}O_{excess}$ can also be influenced by processes of the terrestrial biosphere (Landais et al., 2007) and local conditions (Winkler et al., 2012; Steen-Larsen et al., 2014; Li et al., 2015).

In Switzerland, isotopes in precipitation have been surveyed for decades within the isotope network ISOT by the Climate and Environmental Physics at the University of Bern (CEP), financially supported by the Swiss Federal Office for the Environment (FOEN). The results of this survey are summarised for a west/east transect across Switzerland for three distinct areas representing the Jura Mountains (La Brévine station), the Swiss Plateau (Bern station) and the Southern Alps (Locarno station) (Schürch et al., 2003). The study performed at the Mormont station (Fig. 1) constitutes a prolongation of this transect up to the Tabular Jura that constitutes a flat Plateau to the NW of the last elevation of the Jura Mountains and provides additional information on $\delta^{18}O_p$ and δD_p behaviour preventing the rainout effect that may occur when moisture encounters the first escarpment of the Jura Mountains. The link between $\delta^{18}O$ in precipitation and cave waters has been previously studied in Milandre cave by Perrin et al. (2003a).

In this paper, we present a comprehensive overview of the hydrogen (δD) and oxygen ($\delta^{18}O$ and for the first time $\delta^{17}O$ in drip water and speleothem fluid inclusions) isotope signal in
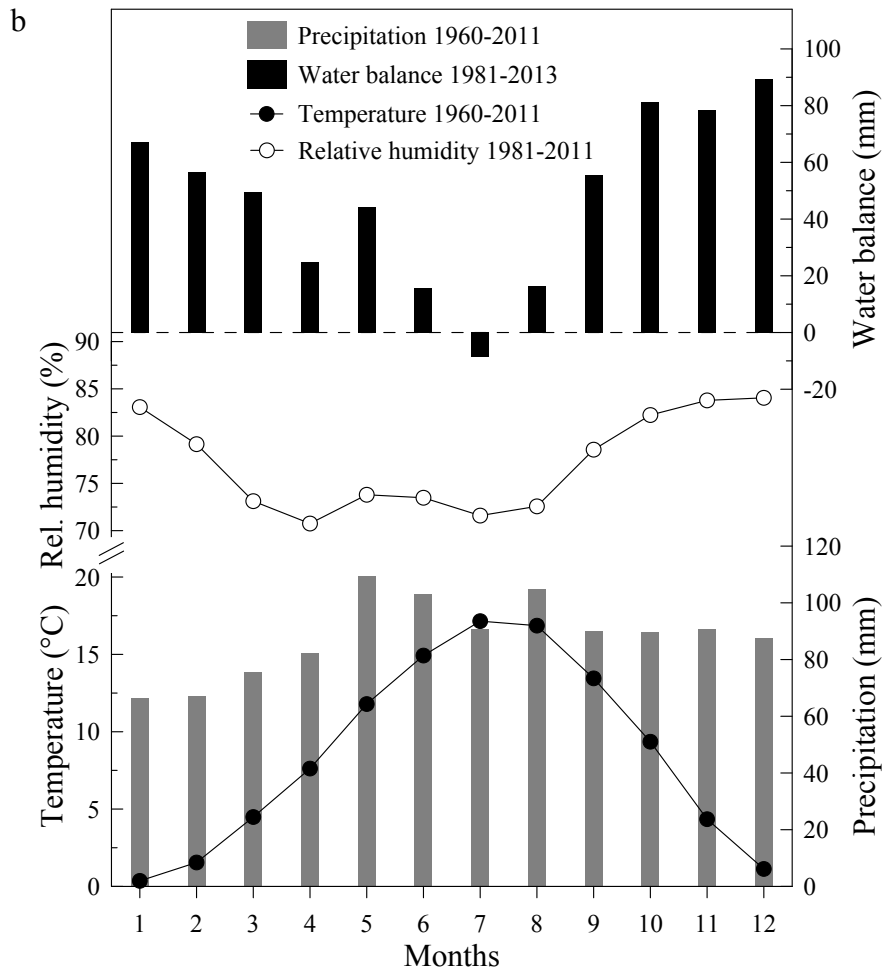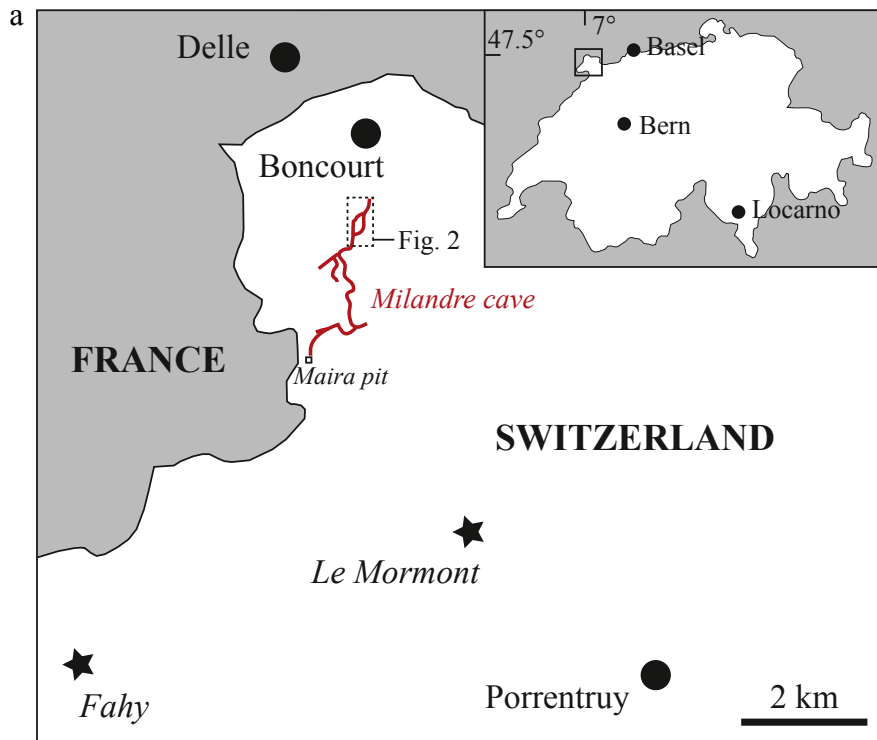
Fig. 1. (a) Milandre cave location (46 km eastward of Basel) with MeteoSwiss stations Le Mormont and Fahy (stars). Isotope network stations (Basel, Bern and Locarno) run by the Climate and Environmental Physics at the University of Bern are displayed in the upper right figure. (b) Annual climatology at MeteoSwiss station Fahy. Mean values for each month are given for precipitation, temperature, relative humidity and water balance (rain − evapotranspiration) for different time intervals. In July, evapotranspiration is larger than the amount of precipitation.

precipitation and karst water in the Jura Mountains. We investigate the isotopic evolution from precipitation to cave drip water and its final enclosure into the speleothem fluid inclusions, and discuss the preservation of the climate signal. Based on these investigations, we conclude that stalagmites from Milandre cave are well suited for future paleoclimate reconstructions.

2. Site settings

Milandre cave (47.4855° N/7.0161° E, elevation 373 m a.s.l.) is located in Boncourt (45 km westward of Basel, NW Switzerland) (Fig. 1). Geologically, the cave is part of a karst aquifer belonging to the Jura Mountains geological structure; more precisely it is located in the Tabular Jura unit that is made of subhorizontal Mesozoic limestones overlying Oxfordian marls. Milandre aquifer consists of a few metres thick soil and epikarst that overlie the unsaturated zone of the karst and eventually the phreatic zone (Perrin et al., 2003b).

The cave section shown on Fig. 2 represents approximately one

third of the total network. Cave galleries develop mostly along fractures oriented north/south on a horizontal distance of 2.7 km with a total of 10.5 km of galleries and an overall positive elevation of 135 m. The 4.633 km long Milandrine River flows in the lower part of the cave system which drains a surface catchment area of around 13 km^2 that is at a mean elevation of 500 m a.s.l. (Perrin, 2003; Perrin et al., 2007). The Milandrine flows directly into the Allaine River after passing a major siphon located at the natural resurgence. Except for this first natural entrance, the cave has a second natural access 30 m above the siphon. A tunnel to access the former show cave has been built close to the natural entrance to facilitate access for visitors, but in the seventies the exploitation was stopped due to major flooding. The former show cave (200 m long) is connected at its end to a well preserved fossil gallery called Galerie des Fistuleuses (literally "soda straws gallery") via a second man-made access tunnel (15 m long) excavated by the Jura caving club and opened in March 1968. A metallic door was placed in this connecting tunnel to preserve the cave site. This entrance remains closed, except for safety reasons when CO$_2$ concentration levels are
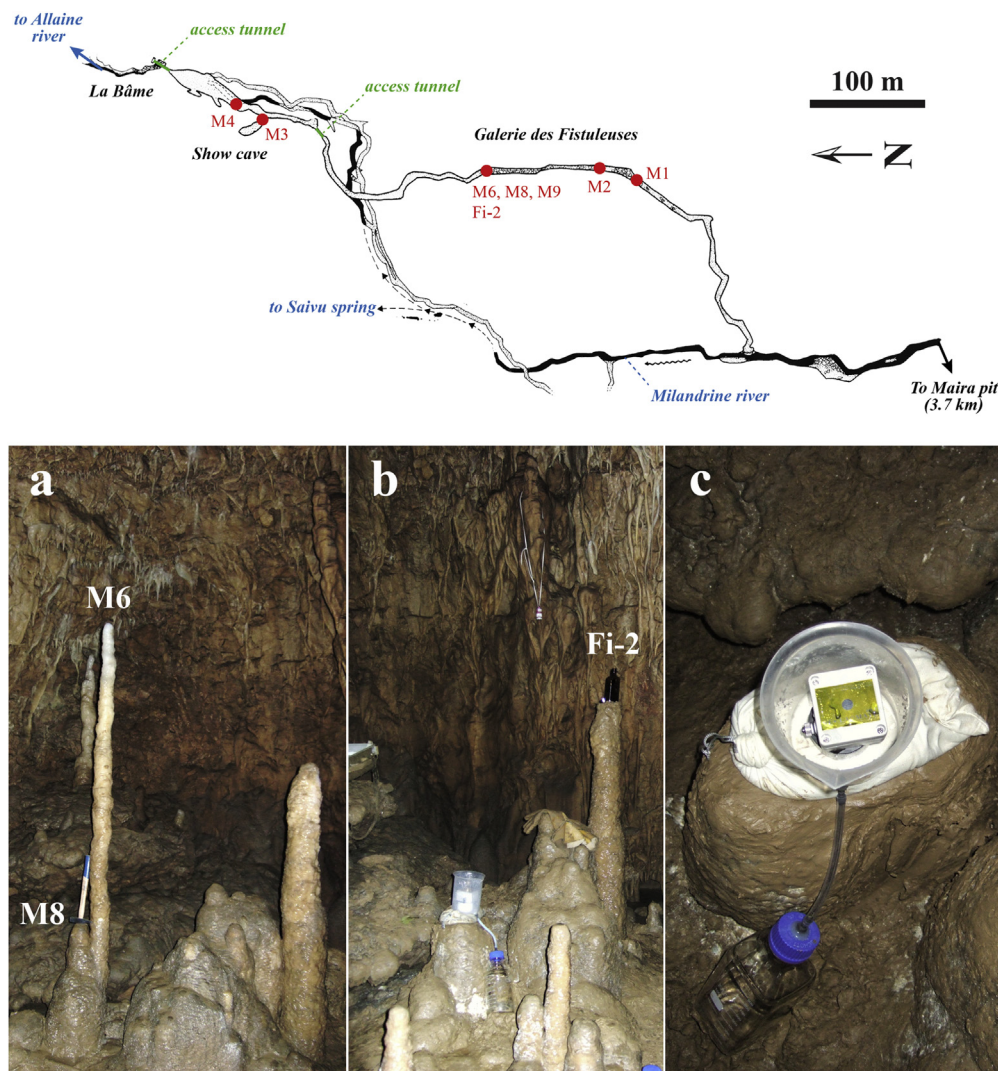

Fig. 2. Topographic map of the downstream part of Milandre cave with locations of collected stalagmites (M1 to M9) as well as drip sites (M2, M4, M6, M9 and Fi-2). The cave continues on 3.7 km to reach the artificial Maira pit (modified from Gigon and Wenger, 1986). The Galerie des Fistuleuses is located ~80 m under the surface and corresponds to a 400 m long oval-shaped tube with an average height of three metres interrupted by two crawling sections. It is part of an upper level of fossil galleries located approximately 30 m above the active Milandrine River. To access the upstream part of the cave a 20 m high pit called Puits du Maira ("Maira pit", Fig. 1) was excavated and inaugurated in 1974. This new excavation allows speleologists to go across the cave. The pictures show the cave chamber with (a) M8 and M6 stalagmites before being removed. (b) General view with M6 and Fi-2 drip sites after removal of stalagmites. (c) Drip logger and water collection system for M6 drip site.

too high to allow scientific exploration. Land use above the cave mainly consists of forests, pastures and isolated individual constructions, especially above the downstream parts including the monitoring site. An extended description of the hydrological settings (Perrin et al., 2003a), epikarst storage characteristics (Perrin et al., 2003b) and hydraulics aspects of Milandre cave system (Jeannin, 1996) allow a good understanding of the system.

Our monitoring study focuses on the *Galerie des Fistuleuses* where most of the stalagmites were collected. Furthermore, it has the main advantage of being easily accessible and that the cave climate is not disturbed when the doors remain closed. A detailed topographic map and an extended description are available in Gigon and Wenger (1986).

The climatic conditions above Milandre cave are representative for Western Central Europe. Annual repartition of moisture fluxes for the northern Swiss Alps gives the following results: ~39.5% from North Atlantic sectors, ~23% from Mediterranean area, ~21% from Europe continental source and ~16.5% from Northern Europe (Sodemann and Zubler, 2010). Moreover, the source of precipitation suggests a principal continental contribution for the summer months whereas during winter continental contribution is low and the North Atlantic represents the major input. Contribution of moisture fluxes coming from the Mediterranean occurs mostly in winter, spring and autumn. For our study site we can expect similar conditions.

Mean annual precipitation recorded at Fahy station (Fig. 1) between 1960 and 2011 averages 1055 mm. An increase of 40 mm between the periods 1960—1990 and 1990—2011 is observed. Moreover, seasonal variability is clearly visible with significantly lower average precipitation amounts (monthly average of 74 mm) in winter (December-January-February, DJF), highest precipitation amount (101 mm) in summer (June-July-August, JJA) and intermediate values (89 mm) in March-April-May (MAM) and September-October-November (SON). Mean annual temperature at Fahy station (2 m above surface) over the last five decades shows maximum values in August with 17.2 °C and minimum in January with 0.4 °C for an overall average air temperature of 8.6 °C. It is worth noting that mean annual temperatures increase from 8.1 °C to 9.2 °C between the period 1960—1990 and 1990—2011, showing a significant warming of the Jura Plateau region. Temperature in the soil (5 cm depth) is also recorded at the station and gives mean annual values of 10.3 °C between 1990 and 2011 which is 1.1 °C higher than the surface temperature.

Correlation maps were developed using the KNMI Climate Explorer (http://climexp.knmi.nl/) and the CRU TS 3.22 datasets (0.5° × 0.5° resolution) for temperature and precipitation (Harris et al., 2014) to investigate the relationship of different climate parameters for NW Switzerland based on available temperature and precipitation (Fahy station, time series 1990—2011) and $\delta^{18}O_p$ (Basel CEP station, time series 1986—2010). According to the approach of Rozanski et al. (1992), seasonality of time series was removed beforehand. For Fahy station, spatial correlation maps with the CRU TS gridded data indicates that the mean annual temperature and precipitation are representative for Western Central Europe, including Switzerland, France (eastern, centre and north), Germany and Belgium. Indeed, local temperature at Fahy station and European temperature are significantly correlated (r > 0.80) for most of central Europe (Fig. 3a). Spatial correlation coefficients between the amount of precipitation in Fahy leads to a significant correlation (r > 0.60) for Western Central Europe (Fig. 3b). Correlation maps between $\delta^{18}O_p$ in Basel CEP station and temperature show significant correlation (r = 0.60, Fig. 3c) with Western Central Europe (e.g. Germany, France and Belgium), whereas no correlation is observed with the amount of precipitation (Fig. 3d).

3. Methodology

3.1. Monitoring

Cave monitoring was carried out in the *Galerie des Fistuleuses* between November 2011 and June 2014. Continuous and spot measurements of cave temperature, drip rate, relative humidity and air P_{CO2} measurements were conducted. Cave air temperature was measured every 15 min since October 2012 using UTL-3 Scientific Dataloggers (GEOTEST, Zollikofen and Snow and Avalanche Research SFL, Davos, Switzerland) at an accuracy of 0.1 °C. A Stalagmate Plus Mk2b (Driptych, United Kingdom) was used to monitor drip rates using an acoustic technique (drops per hour) at the M6 site since June 2012 (Collister and Mattey, 2008). The device was placed in an open pot connected to a 1 L glass vial through an outlet tube to collect the water in glass bottles which were replaced around every three months (Fig. 2).

In the *Galerie des Fistuleuses*, spot measurements show air flow lower than 100 l/s (Testo 405-V1 device), a relative humidity of 100% (Aspirationspsychrometer Hänni device) and P_{CO2} ranging from 0.30 to 1.41% (continuous (CORA device) and spot (Dräger X-am 5600 device) measurements from 2008 to 2014. Occasionally, the P_{CO2} concentration in the gallery can rise up to values of around 4%, especially during late autumn and early spring, as a result of processes that still need to be investigated.

Water samples were collected for geochemical analysis at the sites where stalagmites were taken (Table 1) to better understand isotope behaviour occurring between precipitation, drip water and its enclosure in speleothem fluid inclusions. The survey includes five sites for drip water isotopes (Section 3.2) and three for temperature (including M2, M4, M6, M8, M9 and Fi-2). M6, M8, M9 and Fi-2 are located in the same cave chamber (refer to Fig. 2 for site positions).

Temperature and drip loggers were installed in the chamber where M6, M8 and M9 stalagmites were collected, approximately 300 m after the end of the show cave (Fig. 2). A drip logger was placed at the exact location where water was dripping from a soda straw on M6 stalagmite (from a height of ~2 m). Stalagmite M8 grew close to M6 but was not active when removed. Finally, waters from the three drip sites (M6, Fi-2 and M9 which are 0.5 and 5 m away from M6, respectively) were collected and analysed to estimate the homogeneity of the drip water chemistry.

3.2. Water isotope monitoring program

Isotope data of precipitation are based on two meteorological stations from the MeteoSwiss network. Precipitation samples and daily amount data were obtained from Mormont station (n° 534, 47.44° N/7.04° E, altitude 540 m a.s.l.). The precipitation collection campaign was carried between March 2012 and July 2014, and water of a total of 332 precipitation events was collected at 8 a.m. local time in an open gauge and stored in 100, 200 or 500 ml sealed glass bottles depending on the precipitation amount. One must keep in mind that when collecting in an open gauge, evaporation occurring throughout the day could lead to a fractionation of the precipitation water, especially during the summer. The automated Fahy station (n° 500, 47.42° N/6.94° E, altitude 596 m a.s.l), located 7 km away from Mormont station, has provided daily data of precipitation amounts, mean relative humidity soil and air temperature since 1960. Both stations are located close to Milandre Cave (Fig. 1) and therefore used as reference sites.

In the cave, water samples were collected at M2, M4, M6, M9 and Fi-2 drip sites between November 2010 and June 2014, and are further named "downstream" drip waters. Moreover, additional waters from one secondary intermediate flow tributary of the
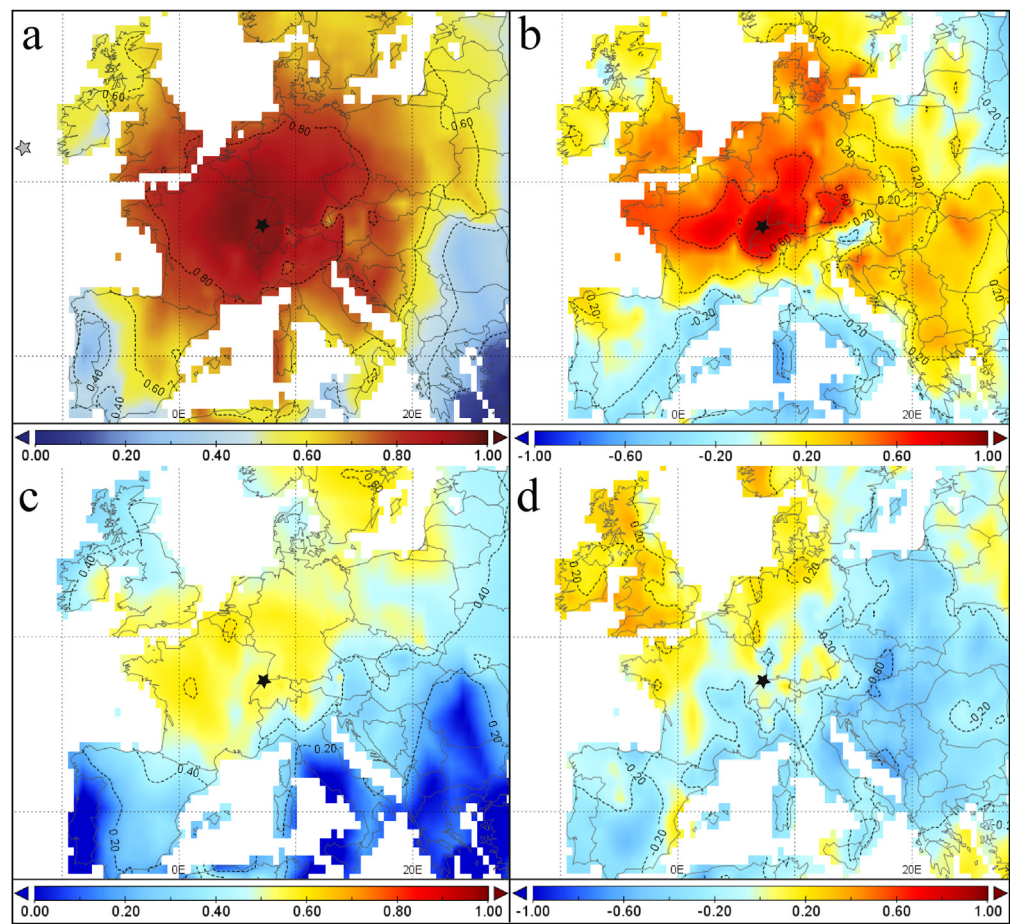
Fig. 3. Spatial correlation maps for Fahy MeteoSwiss (star, plots a and b) and CEP Basel (star, plots c and d) stations. Different correlation coefficient r ranges are given for temperature (0–1) and precipitation (−1 to 1) maps. (a) Correlation of temperature in Fahy MeteoSwiss station versus European temperatures for the period 1990−2011. (b) Idem for precipitation amount against European precipitation amount. (c and d) Correlation between δ^{18}O$_p$ in Basel CEP station with (c) European temperatures and (d) amount of precipitation for the period 1982−2010. The grey star in (a) represents the approximate location of M6 buoy.

Milandrine River (EN) and three additional percolation samples (ST, VI and GO) with approximately five or six orders of magnitude higher flow than M6 were collected for comparison in the upstream part of the cave (Perrin et al., 2003a) and are further called "upstream" cave waters.

3.2.1. Isotope measurements

Water isotope analyses of precipitation and cave waters were performed at the CEP (University of Bern) using a Picarro L2140-i wavelength-scanned cavity ring-down spectroscopy (WS-CRDS) instrument (Picarro Inc., Sunnyvale, CA, USA). For precipitation and drip water analysis, aliquots of water are filled in 2 ml glass vials and sealed with rubber/aluminium caps. The vials are then placed in a PAL COMBI-xt autosampler (CTC Analytics AG, Zwingen, Switzerland) connected to the Picarro L1102-i for δD and δ^{18}O and

L2140-i for additional δ^{17}O values. Water is then injected using a syringe six times directly into the vaporisation unit of the analyser and the three first values are discarded due to memory effect. Reproducibility of measurements is typically 0.1‰ for δ^{18}O and δ^{17}O and 0.5‰−1‰ for δD.

For isotope measurements of fluid inclusion water, we used a new online method based on a Picarro L1102-i WS-CRDS instrument (Affolter et al., 2014) that allows measuring both δD$_{fi}$ and δ^{18}O$_{fi}$ isotopes on a single speleothem sample with precisions better than 0.4‰ for δ^{18}O$_{fi}$ and 1.5‰ for δD$_{fi}$. Furthermore, accuracy and precision of the new method were also successfully assessed through an inter-laboratory comparison with the CF-IRMS method (Meckler et al., 2015). The only modification made to the line is the replacement of the stainless steel capillary connecting the peristaltic pump to the dripping device by a glass capillary (0.18 mm

Table 1
List of collected stalagmites in Milandre cave and related monitored parameters. The isotope parameters are for drip water.

Name	Stalagmite	Active	Collection	Location	Monitored parameters at location
M2	Yes	Yes	2007	Gal. des Fistuleuses	Cave T
M4	Yes	Yes	2007	Show cave	Cave T, δD, δ^{18}O, δ^{17}O
M6	Yes	Yes	2011	Gal. des Fistuleuses	Cave T, drip discharge, δD, δ^{18}O, δ^{17}O
M8	Yes	No	2011	Gal. des Fistuleuses (next to M6)	Cave T
M9	Yes	Yes	2014	Gal. des Fistuleuses (5 m from M6)	Cave T, δD, δ^{18}O, δ^{17}O
Fi-2	No	Yes	growing	Gal. des Fistuleuses (1 m from M6)	Cave T, δD, δ^{18}O, δ^{17}O

inner diameter). A significant improvement was brought to the measurement protocol with a reduction of time from 5 to 2 h (90 min to recover the background condition stability and 20–40 min for the sample measurement itself mainly depending on the amount of released water) for one speleothem sample measurement, allowing up to five sample measurements per day. To perform $\delta^{17}O$ measurements in speleothem fluid inclusions, the line was connected to a Picarro L2140-i that is able to measure $\delta^{17}O$ in addition to $\delta^{18}O$ and δD. The instrument performance was assessed using the same approach as described in Affolter et al. (2014). The precision of $\delta^{17}O$ measurements for stalagmite water samples is 0.3‰. Table 2 summarises the precision of the different water isotope measurements. In this study, blocks of calcite of around 0.5 g were crushed releasing ~0.6 µl of water for fluid inclusions analysis of recent samples (M6), whereas blocks of ~1.5 g where necessary for early Holocene (M8) samples to provide ~0.5 µl. It is worth mentioning that Holocene values are given here only for a first preliminary comparison to present conditions. For isotope analysis of the calcite ($\delta^{18}O_c$), the samples were measured using a Finnigan Delta V Advantage mass spectrometer equipped with an automated carbonate preparation system (Gas Bench II) at the Institute of Geological Sciences, University of Bern, Switzerland. 150–200 µg of sample were analysed and results are reported relative to the international Vienna Peedee Belemnite (VPDB) standard. The analytical error for $\delta^{18}O_c$ is 0.07‰ VPDB (1σ) (Fleitmann et al., 2009).

3.2.2. Isotope calibration and uncertainty

For the measured $\delta^{18}O$ and δD, we follow a four point calibration procedure by using four internal water standards listed in Table 2 (Meerwasser, ST-08, Eiswasser and Bern-SLAP) that are well tighten to the international accepted values of the VSMOW-SLAP scale using the Picarro L2140-i instrument. No such value has been accepted yet for $\delta^{17}O$ by the international community. Therefore, we slightly change the procedure for this parameter. Through $\delta^{17}O$ and $\delta^{18}O$, we have access to $^{17}O_{excess}$ (given in per meg (10^{-6}) due to very small variations) following Luz and Barkan (2010):

$$^{17}O_{excess} = \ln\left(\delta^{17}O + 1\right) - 0.528 \times \ln\left(\delta^{18}O + 1\right) \qquad (1)$$

and consequently:

$$\delta^{17}O(‰) = \left(\left(e^{\left(\frac{^{17}O_{excess}}{10^6} + 0.528 \times \ln\left(\frac{\delta^{18}O}{1000} + 1\right)\right)}\right) - 1\right) \times 1000 \qquad (2)$$

If we set $^{17}O_{excess}$ to zero in Eq. (2), we can calculate $\delta^{17}O$ from $\delta^{18}O$ and can follow the same four point calibration procedure as described for $\delta^{18}O$ above. The calibrated $\delta^{17}O$ is then obtained by adding back the calibrated $^{17}O_{excess}$ according to Eq. (3).

$$^{17}O_{excess,calibrated} = {^{17}O_{excess,measured}}$$
$$- \left({^{17}O_{excess,measured}} \ (Meerwasser)\right)$$
$$- (-3)per \ meg\right) \qquad (3)$$

This adjusted procedure that deviates from Schoenemann's approach leads only to significant differences for extraordinary $^{17}O_{excess}$ values that can be found for instance in the stratosphere.

The $^{17}O_{excess}$ values are expressed to the VSMOW scale corresponding essentially to a single point calibration using Meerwasser that has a value of -3 per meg. This results in non-zero values for VSMOW and SLAP (treated as samples), namely $+3$ per meg and -25 per meg. An evaluation using the approach of Schoenemann et al. (2013) leads to 8 per meg higher values than our evaluation for the latest measurements on Fahy precipitation. Further, an evaluation using a four point (as used for $\delta^{17}O$ and $\delta^{18}O$) instead of a single point calibration for $^{17}O_{excess}$ leads to similar values with an offset of about 6 per meg.

Assuming no covariation exists between $\delta^{17}O$ and $\delta^{18}O$ errors (see Table 2), the measurement precision would be in the order of 360 per meg which is far too high to retrieve paleoclimate information from the archives. Nonetheless, due to its mass dependent properties, both oxygen isotopes are covarying and consequently, even if the individual standard deviation of measurements is high, $^{17}O_{excess}$ can be precisely calculated (Landais et al., 2006; Barkan and Luz, 2007; Schoenemann et al., 2013). Indeed, the few measurements made so far indicate a significantly lower uncertainty when directly evaluating the $^{17}O_{excess}$.

Table 2
(a) Overview of internal standard waters used in this study with corresponding values and uncertainties for the isotopes. (b) Overview of standard deviations (SD) for measurements performed on water (precipitation and drip water) and extracted water (speleothem fluid inclusion) samples for two different instruments (Picarro L1102-i and L2140-i). [+] This assigned value is used for the single point calibration of $^{17}O_{excess}$ [*] Only used for fluid inclusions. [#] See discussion about $^{17}O_{excess}$ measurement precision in section 3.2.2.

	δD (‰)	δ^{18}O (‰)	δ^{17}O (‰)	^{17}O$_{excess}$ (Per meg)	d-excess (‰)
(a) Standard					
Internal standards (assigned values)					
Meerwasser	1.24 ± 0.5	−0.04 ± 0.05	−0.03 ± 0.05	−3[+]	1.6
ST-08	−77.46 ± 0.5	−10.79 ± 0.05	−5.69 ± 0.05	19	8.9
Dye-III[*]	−210.23 ± 0.5	−27.21 ± 0.05	−14.44 ± 0.05	25	7.5
Eiswasser	−274.09 ± 0.5	−35.29 ± 0.05	−18.80 ± 0.05	−8	8.2
Bern-SLAP	−262.96 ± 0.5	−55.21 ± 0.05	−29.14 ± 0.05	412	178.7
DOME-C[*]	−428.26 ± 0.5	−54.18 ± 0.05	−29.04 ± 0.05	−54	5.2
Measured in Bern based on internal standards					
V-SMOW	−0.12 ± 0.5	−0.01 ± 0.05	0.00 ± 0.05	3	0.0
SLAP	−428.74 ± 0.5	−55.56 ± 0.05	−29.76 ± 0.05	−25	15.7
Assigned values after Schoenemann et al. (2013)					
VSMOW	0.00	0.00	0.00	0	0.0
SLAP	−427.50	−55.50	−29.70	0	16.5
(b) Standard deviation					
SD water (L2140-i)	0.5	0.1	0.1	10	0.5
SD extracted water (L1102-i)	1.5	0.4			1.6
SD extracted water (L2140-i)	1.4	0.2	0.3	360[#]	1.5

4. Results and discussion

4.1. M6 drip discharge

Drip rates between 2012 and 2014 at the M6 site are highly variable and range from 11 drops/hour (October 2012, 2013 and 2014) up to 278 drops/hour (February 2013). A seasonal pattern is clearly visible with the highest drip rates during the winter months (DJF) and the lowest during summer and autumn. Nearby Fi-2 drip site was checked at a three month interval and shows that drip rate was five times higher (with a similar seasonality as at M6) which emphasizes the variability in cave environment and the need of local monitoring. Nevertheless, isotope values for both drip sites are similar (Table 3). Drip rate depends on the aquifer recharge, i.e. on the amount of precipitation above the cave. The comparison between drip rate and precipitation is given in Fig. 4 and shows that both are closely related. The lowest drip rates in summer indicate that the overlying reservoir is draining out, as the aquifer is less recharged in summer mainly due to increased evapotranspiration (Fig. 1). Indeed SON, DJF and MAM potentially contribute to a similar degree to the aquifer recharge with 38%, 37% and 21% respectively. Summer months (JJA) contribute only with 4%. Fairly high precipitation in autumn and winter recharges the aquifer and drip rates are increasing steadily, indicating that cold season precipitation (roughly from September to May) contributes to groundwater replenishment above Milandre cave.

We investigated the relationship between heavy rainfall events and cave drip rates in order to evaluate the response time. During summer when the reservoir is at its lowest level a two day-long precipitation event starting on 23.08.2013 (51.1 mm in total) showed only a slight response in drip discharge two days later (from 28 to 30 drops/hour). On 28.07.2013, a precipitation event
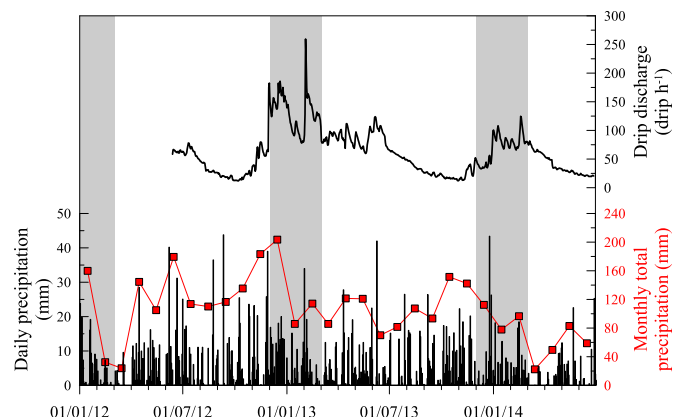

Fig. 4. Daily and monthly precipitation at Mormont MeteoSwiss station between January 2012 and July 2014 and response of the cave system at M6 drip site. Winter seasons (DJF) are highlighted in grey.

(26.5 mm) showed no corresponding signal in the drip discharge but rather a continuous decrease of values. In spring, two consecutive days of precipitation (39.1 mm in total) produced a peak in drip rate (from 64 to 112 drops/hour) around five days later. Another two-day long event starting on 26.04.2013 (total 34.2 mm) gave a response six days later with an increase from 60 to 97 drops/hour. During winter months, an intense precipitation period lasting from 24.12.2013 to 28.12.2013 (85.2 mm in total) led to an increase from 41 to 103 drops/hour around six days later. Overall, drip rates respond within 2−6 days to major precipitation events and drip rate is much more reactive in intensity during colder months (30−60 drops/hour) compared to summer (~0−2 drops/hour).

Table 3

Summary of water isotope measurements for precipitations, cave waters and speleothem fluid inclusions along with standard deviations between measurements (analytical error for speleothem). Measurements are reported relative to the Bern internal water standards that are themselves calibrated to VSMOW and normalised to VSMOW − SLAP.* Based on monthly mean values.# See discussion about $^{17}O_{excess}$ measurement precision in section 3.2.2.

Sample	Time interval	n	δD (‰)	SD (‰)	δ^{18}O (‰)	SD (‰)	δ^{17}O (‰)	SD (‰)	$^{17}O_{excess}$ (Per meg)	SD (Per meg)	d-excess (‰)	SD (‰)
Precipitation stations												
Basel CEP*	July 12 − June 13		−70.33	26.24	−9.88	3.27					8.71	1.04
Bern CEP*	July 12 − June 13		−78.86	29.67	−11.05	3.54					9.56	2.25
Locarno CEP*	July 12 − June 13		−61.20	28.57	−9.07	3.52					11.4	2.83
Mormont	July 12 − June 13	149	−68.30	34.77	−9.68	4.32	−5.10	2.29	19	14	9.10	4.72
Mormont	July 13 − June 14	125	−60.99	31.33	−8.31	4.05	−4.39	2.15	16	17	5.51	6.28
Mormont	July 12 − June 14	274	−64.97	33.38	−9.05	4.25	−4.78	2.25	18	15	7.47	5.76
Mor. weighted	July 12 − June 13	id.	−73.91	id.	−10.43	id.	−5.50	id.	19	id.	9.52	id.
Mor. weighted	July 13 − June 14	id.	−67.13	id.	−9.17	id.	−4.83	id.	17	id.	6.16	id.
Mor. weighted	July 12 − June 14	id.	−71.03	id.	−9.89	id.	−5.22	id.	18	id.	8.10	id.
«Downstream» drip waters												
M6	June 12 − June 14	7	−60.33	1.62	−8.73	0.13	−4.60	0.07	18	9	9.52	0.69
Fi-2	June 12 − June 14	7	−61.69	2.31	−8.83	0.25	−4.65	0.13	19	12	8.93	0.96
M9	Oct. 13 − June 14	4	−61.32	3.10	−8.67	0.43	−4.56	0.22	26	15	8.05	1.12
M4	June 13 − Jan.14	2	−62.11	1.02	−9.00	0.11	−4.74	0.05	24	7	9.85	0.15
M2	Jan. 13 − Jan. 14	1	−58.49		−8.62		−4.56		−1		10.45	
«Upstream» cave waters												
EN	Sept. 12 − April 14	8	−63.29	1.97	−9.04	0.23	−4.78	0.11	8	11	9.06	0.70
GO	Sept. 12 − April 14	8	−61.77	1.25	−8.94	0.12	−4.72	0.06	12	10	9.76	0.68
ST	Sept. 12 − April 14	8	−62.22	2.20	−8.92	0.25	−4.72	0.12	5	14	9.17	0.60
VI	Sept. 12 − April 14	8	−59.06	0.98	−8.43	0.23	−4.45	0.12	8	9	8.40	2.53
Speleothem fluid inclusions												
M6 top 4	0-40 years	1	−60.1	1.5	−8.9	0.2	−4.8	0.3	36	360#	11.1	1.5
M6 top 5	0-40 years	1	−60.3	1.5	−8.3	0.2	−4.7	0.3	−15	360#	6.1	1.5
M8-4	Early Holocene	1	−63.0	1.5	−9.4	0.4					12.2	1.6
M8-4bis	Early Holocene	1	−61.6	1.5	−9.8	0.2	−5.2	0.3	127	360#	16.8	1.5
M8-5	Early Holocene	1	−62.3	1.5	−7.5	0.4					2.3	1.6
M8-5bis	Early Holocene	1	−63.1	1.5	−8.0	0.2	−4.4	0.3	23	360#	0.9	1.5
M8-6	Early Holocene	1	−65.7	1.5	−7.7	0.4					4.1	1.6
M8-6bis	Early Holocene	1	−65.6	1.5	−10.3	0.2	−5.6	0.3	39	360#	16.8	1.5

Indeed, heavy rainfall events in summer seem to produce no or only slight changes in drip rates, which can be explained by the fact that the water is evaporated at the surface and used by vegetation and only lastly for the refilling of the soil and epikarst.

While drip loggers count the total number of drops that fall from the roof in the cave, the drops are collected in a bottle for subsequent analysis of water isotopes. Knowing the collected amount of water between two visits and the total drip amount over the same period, we estimated drop size diameter on two consecutive 3 month intervals between July 2013 and January 2014. We obtained similar results with respectively drop size diameters of 2.769 mm (91855 drops, 1021 g of water collected) and 2.763 mm (89755 drops, 990.8 g) for an averaged drop volume of 11.08 mm^3 (or μl). This would correspond to a mean discharge of 0.13 μl/s.

4.2. Mean annual surface and cave temperatures

Comparison between cave, soil and atmospheric temperature is shown in Fig. 5 to determine if the cave temperature corresponds to the mean temperature at the surface (Luetscher and Jeannin, 2004). A temperature logger was placed at the M6 drip site location and has recorded cave temperatures from 24th October 2012 and is still running. A one year average (October 2012−October 2013) shows a mean annual temperature in the cave of 9.8 ± 0.2 °C with minimum and maximum temperatures of 9.0 °C and 10.2 °C, where extremes could probably be due to the opening of the door connecting the show cave and the *Galerie des Fistuleuses* to allow cave CO_2 concentrations to decrease. For the same period, surface mean annual temperature at Fahy station recorded an average temperature of 8.5 °C, slightly colder (ΔT = −1.3 °C) than mean cave temperature. The difference towards warmer temperatures in the cave can be explained by the 200 m elevation difference between the cave (~400 m a.s.l.) and Fahy station (~600 m a.s.l.). It should be noted that previous temperature monitoring performed between 2008 and 2010 in the same cave gallery (Schmassmann, 2010) showed consistent mean annual values of 9.6 °C. Consequently,
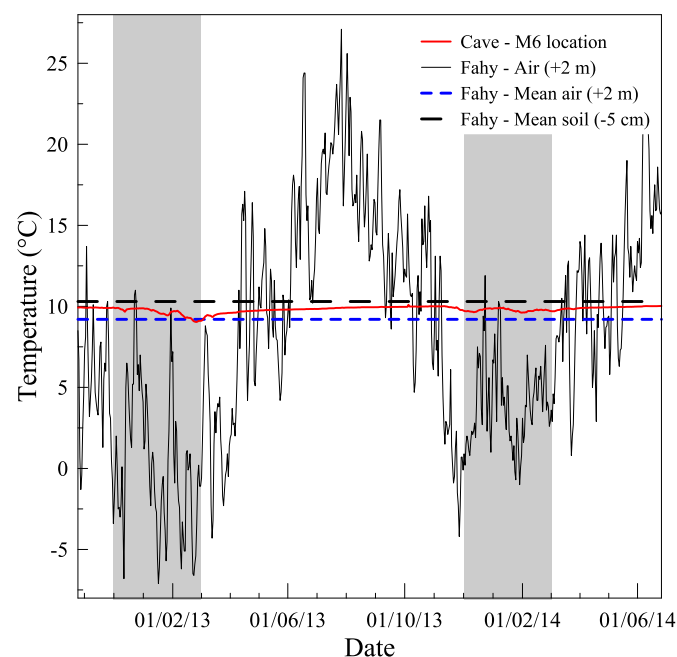

Fig. 5. Cave air temperature is included between mean air temperature and soil temperature when compared to Fahy station (~200 m higher than the monitored cave chamber). Small variations in cave air temperature are probably due to the opening of the doors to ventilate the cave for CO_2 dissipation. Winter seasons (DJF) are highlighted in grey.

observations are similar over both monitoring periods and mean annual cave temperature corresponds to the mean annual surface temperature when taking the adiabatic gradient of ~0.0055 °C/m (Rolland, 2003) into account.

4.3. Comparison of water isotopes in precipitation, drip water and speleothem fluid inclusions

The potential of Milandre stalagmites for paleoclimate reconstruction use can be estimated by comparing fluid inclusion water isotopes to that of the corresponding drip water and amount weighted precipitation. Table 3 summarises δD, $\delta^{17}O$, $\delta^{18}O$ stable isotopes results and associated second order proxies d-excess and $^{17}O_{excess}$ performed in this study. In total, 332 analyses of precipitation, 22 "downstream" drip waters, 32 "upstream" cave waters and 8 fluid inclusions (including 4 without $\delta^{17}O$) were performed.

Isotopes in drip water are integrated over a long period of time (see section 4.8) and consequently, precipitation values must be given in mean weighted delta value form using Eq. (4) to allow comparison with cave drip isotope values:

$$\delta i_{\text{mean weighted}} = \frac{\sum\limits_{i} \delta_{i \times n_i}}{\sum\limits_{i} n_i} \qquad (4)$$

where δ_i is the daily precipitation isotope value and n_i the daily amount of precipitation. Mean weighted values are given in Table 3. It is noteworthy that a net recharge weighting does not alter the data significantly. Isotope values are always given in brackets in this specific order (δD; $\delta^{18}O$; $\delta^{17}O$). Values are sometimes given for seasons: winter (DJF), spring (MAM), summer (JJA) and autumn (SON).

4.3.1. Isotopes in precipitation

Precipitation above Milandre catchment area shows δD_p and $\delta^{18}O_p$ values with a typical local signature comparable to values obtained for Switzerland (Perrin et al., 2003a; Schürch et al., 2003). Fig. 6 summarises all measurements of daily precipitation together with their respective $^{17}O_{excess}$ and d-excess, temperature and relative humidity for Mormont station.

Variability of isotope values in precipitation is high, with values ranging between −1.07‰ and −165.63‰ for δD_p, 3.36‰ and −21.75‰ for $\delta^{18}O_p$ and 1.79‰ and −11.49‰ for $\delta^{17}O_p$ with corresponding mean isotope composition between July 2012 and June 2014 of (−64.97; −9.05; −4.78) ‰. Isotope values show a seasonal pattern with enriched values in JJA (−41.17; −6.03; −3.18) ‰ and depleted in DJF (−86.40; −11.82; −6.23) ‰ with corresponding amplitudes (45.2; 5.8; 3.1) ‰. Mormont shows large variations for two consecutive years with a shift of (7.31; 1.37; 0.71) ‰. However, an average of four years show significantly damped variations that do not exceed 0.5‰ in $\delta^{18}O_p$ at Bern CEP station.

CEP stations values are given for comparison and correspond to the transect Basel-Bern-Locarno in Switzerland (Figs. 1 and 8b). Locarno is located on the southern side of the Alps and presents different climatic settings from Bern and Basel located on the northern side. Basel station is close to Mormont station and presents slightly more negative values of 0.2‰ and 2‰ for $\delta^{18}O_p$ and δD_p respectively.

4.3.2. Isotopes in cave waters

Drip waters show comparable values for all three isotopes between "downstream" drip sites and "upstream" cave waters with overall means of (−61.14 ± 1.56; −8.80 ± 0.20; −4.64 ± 0.11) ‰. Slight differences may have to do with the heterogeneity of the sampling time and natural local variability. In the monitored chamber, values for M6 (−60.33; −8.73; −4.60) ‰ are integrated
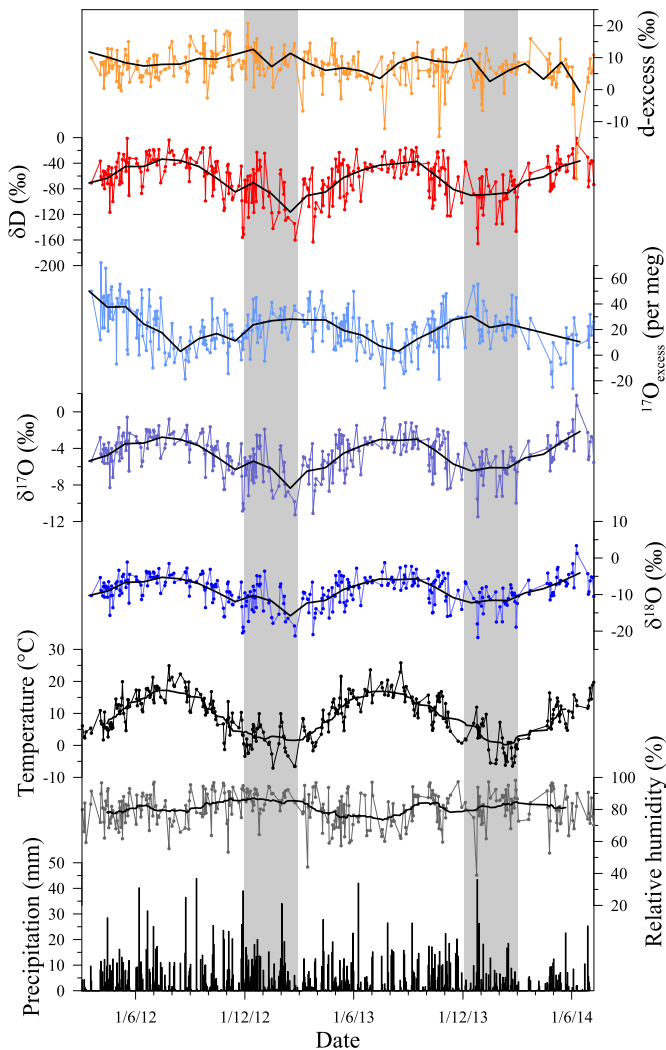
Fig. 6. Water stable isotope measurements on daily precipitation events (coloured circles) and corresponding monthly means (black lines) in precipitation from Mormont station together with temperature and relative humidity from Fahy station (black and grey circles) and their respective 31 days running averages (black lines). Winter seasons (DJF) are highlighted in grey. (For interpretation of the references to colour in this figure legend, the reader is referred to the web version of this article.)

over three months (around 1 L sample), whereas spot values are given for Fi-2 (around 10–20 ml samples). Their isotope values are almost identical, with shifts of 1.4‰ in δD_{dw} and 0.1‰ in $\delta^{18}O_{dw}$ over the two years. The overall amplitude is 0.4‰ for $\delta^{18}O_{dw}$. A seasonal trend is visible but with two major differences compared to the precipitation signal: (i) the signal amplitude is smoothed by a factor of ~25 and (ii) the signal is shifted of several months due to the residence time in the karst (see section 4.8 for discussion).

In summary, waters sampled at different cave sites show comparable means, amplitudes, as well as standard deviations in their isotopic compositions implying that the precipitation waters are homogeneously mixed in the soil, epikarst and vadose zone above the cave before being transferred to the cave drip sites.

4.3.3. Isotopes in fluid inclusions

For fluid inclusions, some results from modern active samples covering the last 40 years were published previously (Affolter et al., 2014) and additional measurements are given in Table 3. Speleothem fluid inclusion values for recent samples (−61.3; −8.3; −4.7) ‰ are similar for δD, $\delta^{18}O$ as well as $\delta^{17}O$ to the cave drip water

suggesting that signal coming from the cave drip water is faithfully recorded in the speleothem fluid inclusion water. For the early Holocene sample values are slightly more negative but still comparable to today's values.

4.4. Second order parameters d-excess and $^{17}O_{excess}$ between precipitation, drip water and speleothem fluid inclusions

In the daily precipitation samples from Mormont, $^{17}O_{excess}$ values vary from −26 to 72 per meg for a two years mean value of 18 per meg (idem for weighted mean) similar to the two years averaged drip water values of 18 and 19 per meg for the M6 and nearby Fi-2 drip sites in the monitored cave chamber. Mean seasonal values are 13 per meg (JJA), 17 per meg (SON), 25 per meg (DJF) and 19 per meg (MAM). During the monitoring period, $^{17}O_{excess}$ shows recurrent trends with rather stable winter values of 27 ± 2 per meg (December 12 − April 13) and 25 ± 4 per meg (November 13 − March 14) and minimum values of 3 per meg for both August 2012 and August 2013. The former may be explained by the rather constant moisture source originated from Atlantic Ocean during winter months (Sodemann and Zubler, 2010). Overall, $^{17}O_{excess}$ shows a monthly amplitude of 40 per meg which is comparable to observations made on a yearly basis at Vostok station in Antarctica (Landais et al., 2012a). In Fig. 6, $^{17}O_{excess}$ is anti-correlated to $\delta^{18}O_p$ and consequently with site temperature with more positive values in winter (40 per meg) and lower values in summer (0 per meg). Long term $^{17}O_{excess}$ time series records in precipitation are rare in low latitudes making the comparison difficult. Nevertheless, a few records are available but mainly in the Polar Regions and there, our observed anticorrelation between $\delta^{18}O_p$ and $^{17}O_{excess}$ is in opposition with the strong correlation observed on a limited number of events in Vostok solid precipitation that was explained by change in the kinetic vs. equilibrium fractionation proportion (Landais et al., 2012a), but similar to what was observed in a snow pit at the same station where the anticorrelation between $^{17}O_{excess}$ and $\delta^{18}O$ may be attributed to stratospheric influences (Winkler et al., 2013). Furthermore, our measurements are in agreement with a few measurements in Greenland described in Landais et al. (2012b). Additionally, in the African monsoon precipitation, Landais et al. (2010) also show an anticorrelation between δD_p and $^{17}O_{excess}$ measured on a very limited amount of precipitation events.

The observed anticorrelation and seasonal variations in $^{17}O_{excess}$ is the result of changing contributions from kinetic and equilibrium fractionation. The equilibrium fractionation factor $\alpha_{equilibrium}$ (slope) for vapour−liquid water is 0.529 (Barkan and Luz, 2005), whereas the diffusion fractionation (kinetic) factor for water vapour is 0.518 (Barkan and Luz, 2007). Thus, the slope determined in meteoric water is a combination of both equilibrium and kinetic fractionation and the corresponding GMWL for oxygen isotopes has a slope of 0.528 (Luz and Barkan, 2010). Based on our own two year record, the averaged α_{mean} is 0.5269 ± 0.0007 (see section 4.7.2) and presents seasonal variations. The fractionation factor is lower in summer (0.5255 ± 0.0009) than in winter (0.5271 ± 0.0004), whereas it is 0.5283 ± 0.0029 and 0.5274 ± 0.0004 for spring and autumn respectively. It is interesting to see that the α_{mean} is close to α_{winter}. It is then possible to formulate an explanation for the anticorrelation between $\delta^{18}O_p$ and $^{17}O_{excess}$ values by seasonal variations in the kinetic fractionation. Indeed, replacing the fractionation factor α in Eq. (1) for summer (low value) will decrease the $^{17}O_{excess}$ values, whereas it is the opposite for winter. Spring values also show a higher $^{17}O_{excess}$ than autumn (Fig. 6) but very close to the mean observed value for precipitation. This might indicate that the mean $^{17}O_{excess}$ value of about 20 per meg observed in our precipitation may correspond to a mean source effect,

according to Uemura et al. (2010) to a normalized humidity of around 65%, which is, however, rather low compared to measured conditions over the Atlantic region even assuming a sea-air temperature difference of 0.5—1 °C (Singh et al., 2005). Mechanisms responsible for these variations should be further studied and include kinetic fractionation during evaporation at the source, during transport, during cloud processes including supersaturation and finally process at the site of precipitation. These mechanisms are complex and involve several meteorological parameters such as humidity, temperature, pressure pattern driving wind fields and strengths, condensation nuclei concentration and its specificity.

To better understand the factors influencing $^{17}O_{excess}$ at the study site, we evaluate its sensitivity to temperature and relative humidity both at the study site and at the main moisture source location. We used the relative humidity and temperature data from the M6 buoy in the North Atlantic (Irish Weather Buoy Network, http://data.marine.ie) located on the west coast of the United Kingdom (53.07°N/15.88°W, see Fig. 3 for approximate location) at a distance of roughly 1800 km to determine if any influence of moisture source coming from the Atlantic can be detected in this remote continental location. Based on a 31 days running average, we first compared $^{17}O_{excess}$ with the temperature or relative humidity. We found that $^{17}O_{excess}$ anticorrelates both with temperature at the study site ($R^2 = 0.36$) and with sea surface temperature ($R^2 = 0.60$). For the relative humidity, $^{17}O_{excess}$ anticorrelates for the Atlantic ($R^2 = 0.22$) but no correlation is observed with local relative humidity ($R^2 = 0.02$) indicating an influence of both temperature and relative humidity of the moisture source. A multiple regression of $^{17}O_{excess}$ with the relative humidity and the temperature at Fahy MeteoSwiss station gives a correlation of 0.41 (R^2). Adding the relative humidity of the Atlantic source region to the regression analyses, the correlation coefficient increases to 0.61 (R^2) and no further improvement is observed when adding the Atlantic source temperature at M6 ($R^2 = 0.62$). It should be noted that even if the monthly running average may introduce an artificially high correlation, this indicates that oceanic condition at the source (M6 buoy) has an influence on $^{17}O_{excess}$ data in NW Switzerland. Further investigations are certainly necessary to disentangle the influence of individual parameters on the $^{17}O_{excess}$. It is nonetheless worth mentioning that the high correlation with the study site may be the reflection of seasonal covariation of temperature ($R^2 = 0.72$) between the oceanic source and the study site, whereas the correlation is low between the respective relative humidity ($R^2 = 0.14$).

Local d-excess shows seasonal fluctuations ranging between −27.96‰ and 21.95‰ around a mean value of 7.41‰ and presents lower d-excess during the summer (~4.7‰) and higher values during winter (~10.6‰). Overall, d-excess shows a seasonal amplitude of 8‰. Differences can be explained by the origin of moisture during the summer that is mainly continental and probably with local secondary evaporation, whereas during winter moisture is mainly provided by the Atlantic Ocean (Sodemann and Zubler, 2010). Schotterer et al. (2000) assigned these variations to evaporation conditions at the moisture source, to evaporation of falling rain-drops and evaporation of local soil moisture. Averaged local weighted d-excess is 8.1‰ in precipitation (7.1‰ in summer and 8.1‰ in winter) and slightly lower compared to drip waters with values ranging between 8.9‰ (M6) and 9.5‰ (Fi-2) for the monitored cave chamber. The 1‰ difference between precipitation and drip water is probably due to the buffering in the karst system resulting from the mixing and residence time and consequently the unequal reservoir filling with more water supplies from the cold season.

In summary, $^{17}O_{excess}$ signal is kept in the drip water whereas d-excess is depleted by ~1‰. That means that sufficient analytical precision and the use of replicates in speleothem fluid inclusion measurements should allow retrieving climate information from both second order parameters from this cave. Indeed, even with a high uncertainty, the range of measured $^{17}O_{excess}$ values from stalagmites (Table 3) is in most cases compatible with the range of precipitation measurements, and even closer to the precipitation value for the modern samples based on two replicates (Table 4). These preliminary results are promising but a larger $\delta^{17}O$ measurement campaign should be initiated to draw more robust conclusion.

4.5. Summary for the monitored chamber

Table 4 summarises the delta values, d-excess and $^{17}O_{excess}$ that are of interest for the monitored cave chamber (M6, Fi-2 and M9). The difference between the Mormont weighted mean and the drip water values is discussed in section 4.8. It is worth mentioning here that if the isotope values are weighted using the net recharge (rain − evapotranspiration) at Fahy station, then values (−73.30‰, −10.20‰ and −5.38‰ for δD_p, $\delta^{18}O_p$ and $\delta^{17}O_p$, respectively) are still close to the precipitation amount weighted. Drip water and sub-recent speleothem fluid inclusion values are similar for δD, whereas for $\delta^{18}O$ and $\delta^{17}O$ values are slightly more negative by 0.4‰ and 0.1‰ respectively but still within the analytical uncertainties. Nevertheless, the two recent sample measurements made with the Picarro L2140-i show identical values (−60.2; −8.6; −4.7) ‰ as M6 drip site. Thus, no significant differences are found between speleothem fluid inclusion water and modern drip water. Early Holocene values show slightly more negative values. For second order parameters, $^{17}O_{excess}$ shows the same value in the cave and in precipitation while d-excess is 1‰ more positive in precipitation. In fluid inclusions, $^{17}O_{excess}$ is potentially preserved and thus, it could be possible to derive

Table 4

Water isotope comparison between precipitations, drip water and speleothem fluid inclusions at M6 drip site. Refer to Table 3 for reproducibility. For recent speleothem samples values were partially published in Affolter et al. (2014).* Measured with Picarro L2140-i.

Water type	Time period	n	δD (‰)	$\delta^{18}O$ (‰)	$\delta^{17}O$ (‰)	$^{17}O_{excess}$ (Per meg)	d-excess (‰)
Precipitation station							
Mormont weighted	July 12 − June 14	274	−71.0	−9.9	−5.2	18	8.1
Cave drip waters							
M6	June 12 − June 14	7	−60.3	−8.7	−4.6	18	9.5
Fi-2	June 12 − June 14	7	−61.7	−8.8	−4.7	19	8.9
Speleothems							
Fluid inclusions	0−40 years	4/2*	−61.3	−8.3	−4.7*	10*	8.6*
Fluid inclusions	Early Holocene	6/3*	−63.6	−8.8	−5.0*		
Speleothem calcite	0−40 years	1		−6.5			
Speleothem calcite	Early Holocene	3		−6.6			

additional information on past biospheric activity when combined with δ^{13}C measurements (Landais et al., 2007) or past hydrological changes (Schoenemann et al., 2014).

Theoretical values for modern speleothem calcite determined using the equation of Friedman and O'Neil (1977) are not far from the $\delta^{18}O_c$ measured values (6.5‰). Indeed, a calculated $\delta^{18}O_c$ value of -7.27‰ is obtained (offset of ~0.8‰) when using the two year $\delta^{18}O$ averaged drip water isotope value of -8.7‰ and cave temperature of 9.8 °C. By doing the same exercise using the most recent empirical relationship based on a large set of cave studies that already take into account a "mean" disequilibrium inherently present in cave environment (Tremaine et al., 2011), a theoretical $\delta^{18}O_c$ value of -6.85‰ is obtained that is even closer to the measured value meaning that $\delta^{18}O_c$ precipitates in disequilibrium. It is interesting to note that in B7 cave in West Germany (Niggemann et al., 2003) located around 450 km northward from Milandre cave $\delta^{18}O$ values of drip water (-8.4‰) and corresponding calcite (-6.3‰) are very similar to those observed in Milandre cave.

The good agreement between the isotopic composition of drip and recent fluid inclusion water confirms that the cave signal is well preserved in speleothems. Nevertheless, δD_{fi} values seem to be a more conservative proxy for paleoclimate reconstructions than the corresponding $\delta^{18}O_{fi}$ values, most likely because hydrogen has no reservoir for isotope exchange during the transfer in the karst whereas oxygen may exchange continuously with the host calcite. During isotope measurements, mixing and storage of the isotopes in the soil and epikarst will allow recovering the decadal mean when measuring speleothem fluid inclusions and the annual mean for $\delta^{18}O$ of the calcite, or potentially seasonal variations. For fluid inclusions this is not an issue since the thickness of samples allows only reconstructions of decadal integrated values in this cave. Indeed, slabs of up to 5 mm thick are required for fluid inclusion analysis and consequently, the time resolution is dependent on the stalagmite growth rate. For example, the modern part of M6 stalagmite exhibits a growth rate of 0.1 mm (laminae counting; Häuselmann, 2013) that would correspond to a resolution of 40—50 years for fluid inclusion measurements done on a 5 mm slab.

4.6. Factors influencing isotope ratios in water

In order to identify the factors influencing stable isotopes in water, we investigated relationships between atmospheric parameters and isotope values. Correlations (R^2), respectively slopes, are always given in brackets and in this specific order (δD; $\delta^{18}O$; $\delta^{17}O$), respectively (d-excess; $^{17}O_{excess}$) for second order parameters.

Correlations of water isotopes in precipitation with daily average temperature are lower (0.28; 0.36: 0.30) than for monthly mean precipitation (0.75; 0.73; 0.73) showing clearly the temperature dependence of the site. Corresponding slopes on a monthly basis (3.26; 0.39; 0.22‰/1 °C) are lower than the 0.56‰/1 °C for $\delta^{18}O$ observed for the region of Bern during the period 1994—2001 (Schürch et al., 2003), but in accordance to the values determined in Basel of 0.34‰/1 °C for the period 1986—2010 which indicates that Basel CEP station is more representative for the Milandre cave area compared to Bern. Low correlations are observed for d-excess and $^{17}O_{excess}$ with local temperature on a daily basis (0.04; 0.06) as well as on a monthly basis (0.03; 0.20).

Relative humidity at the precipitation site shows low correlation for all isotopes (0.04; 0.12; 0.04) and a slightly better correlation with monthly mean relative humidity (0.15; 0.17; 0.17). Second order parameters have no significant correlation both on a daily (0.00; 0.01) and monthly basis (0.08, 0.01). Precipitation amount shows no correlation with all three isotopes both on a daily and on a monthly basis. The d-excess and $^{17}O_{excess}$ show insignificant
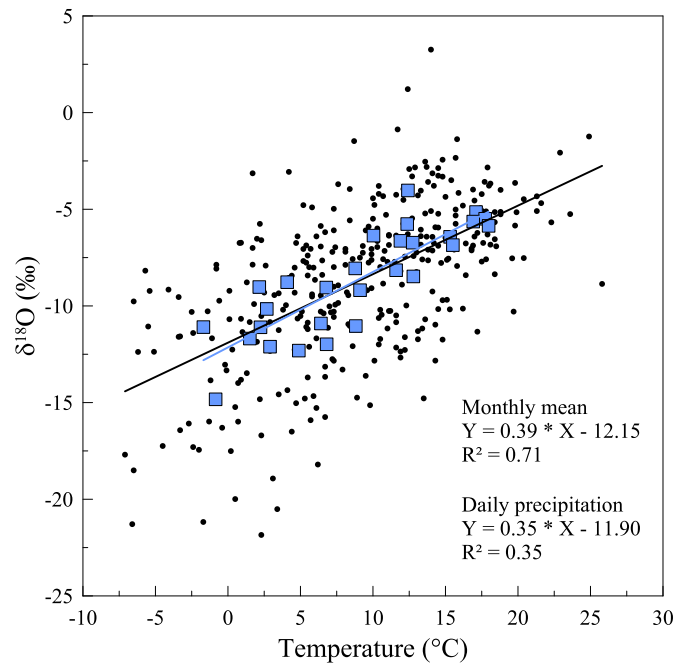

Fig. 7. Relationship between $\delta^{18}O_p$ and temperature for Mormont MeteoSwiss station. Daily precipitation values (black dots) show a lower correlation than monthly mean values (blue squares). (For interpretation of the references to colour in this figure legend, the reader is referred to the web version of this article.)

correlation on a daily (0.09; 0.05) and monthly basis (0.15; 0.07).

Seasonality of stable isotopes in precipitation for Switzerland was shown to be correlated to temperature and water vapour pressure with lower values in winter corresponding to depleted isotope values (Schürch et al., 2003) which is confirmed by our observations (Figs. 7 and 3c). When values are integrated on a monthly basis, all three isotopes react in the same way to temperature (~73%) and to relative humidity (~17%), whereas on a daily basis relationships are less robust. The best correlation for $^{17}O_{excess}$ explains 20% of its variation by site temperature. For d-excess a low correlation of 15% is observed with the monthly amount of precipitation.

In Europe, several monitoring studies were carried out to understand the relationship between water isotopes in precipitation and corresponding cave drip waters. Approximately on a North South transect, in Han-sur-Lesse cave (Belgium), van Rampelbergh et al. (2014) found that the temperature effect has a clear influence on the regional water isotope composition in precipitation with increasing values in summer, similar as observed in this study which is also corroborated with the spatial correlation maps observations (Fig. 3c). Moreover, the water isotope composition of the drip water is constant, suggesting a good mixing and a long residence time in the epikarst above Han-sur-Lesse cave. Nevertheless, the temperature is not always the driving parameter for $\delta^{18}O_p$; for instance, in Villars cave (South France), Genty et al. (2014) observed only a weak correlation between surface temperature and $\delta^{18}O_p$ mainly due to the interaction of different air masses coming from the Atlantic and the Mediterranean Sea. In Molinos cave (North East Spain), Moreno et al. (2014) observed that temperature and amount of precipitation have an important effect on $\delta^{18}O_p$ but the source effect is dominant on $\delta^{18}O_p$ as the cave receives moisture from the North Atlantic and Western Mediterranean which have a distinct $\delta^{18}O$ signature. These three European examples illustrate cave to cave variations in water isotope interpretation and thus, the uniqueness of each cave site and the need for specific cave

monitoring.

Larger scale atmospheric effects can also have an influence on $\delta^{18}O_p$ at the study site. The link between $\delta^{18}O_p$ and the large scale atmospheric patterns such as the North Atlantic Oscillation (NAO) for Europe has been investigated by Baldini et al. (2008) who observed that for central European mid-latitudes the NAO index is correlated to the winter $\delta^{18}O_p$ and this was attributed to the strong control of air temperature on $\delta^{18}O_p$. The NAO is strongly correlated to temperature and precipitation over Europe (Hurrell and Van Loon, 1997) and has consequently a direct influence on $\delta^{18}O_p$ through wind dominant patterns and thus the amount of precipitation and temperature in winter (Baldini et al., 2008). Generally, isotopic values are depleted in winter compared to summer months and the influence of NAO on climatic conditions during the winter months may lead to an increase in precipitation with less negative values that will smooth the annual means. The influence of the NAO on $\delta^{18}O_p$ in central Switzerland has been discussed by Teranes and McKenzie (2001). They present paleoclimate reconstructions using sediments of Lake Baldeggersee (central Switzerland, alt. 463 m a.s.l.). The lake is located around 100 km eastward from Milandre cave and it was shown that $\delta^{18}O_c$ at that site is mainly driven by temperature but it is also suggested that the NAO may have a discernible influence on the isotopic composition of regional precipitation and that long term trend in the NAO index can explain trends in $\delta^{18}O_c$ in lake sediments data (Teranes and McKenzie, 2001). Other observations linked the $\delta^{18}O$ of continental archives with changes in the NAO in central Europe, for alpine ice cores in the Swiss Alps (Schotterer et al., 2002), and even further East, in $\delta^{18}O_c$ from speleothem from Spannagel cave in Austria (Mangini et al., 2005). More recently, Luetscher et al. (2015) interpret the isotopic composition in speleothems as a proxy for changes in the North Atlantic storm track during the Last Glacial Maximum in the Sieben Hengste cave systems (Swiss Alps). It is worth noting that for the last three examples, the link between archives and NAO or storm track is observed at high elevations in the Alps where sensitivity of continental archives to NAO could be higher as for instance suggested for lake sediments in the Western French Alps (Guyard et al., 2013).

To have a closer look at the precipitation data at our site, we investigated the relationships between $\delta^{18}O_p$ and the NAO index both on a two year interval (daily event basis) at the study site and on a 25 year interval at the CEP station in Basel that has recorded $\delta^{18}O_p$ since 1986 (on a monthly basis). Results indicate no correlation ($R^2 = 0.009$) at the study site between daily NAO index and daily $\delta^{18}O_p$ opposite to what was recently observed in NE Spain (Moreno et al., 2014). This observation seems coherent with regard to the relative distance of the Atlantic moisture source and to the multi-source of moisture air masses (Sodemann and Zubler, 2010). When looking at the correlation between monthly NAO index and $\delta^{18}O_p$ in Basel for the period 1986–2012, no correlation ($R^2 = 0.0002$) is observed. For the summer months (JJA), no correlation is observed as expected for both periods with $R^2 = 0.005$ and $R^2 = 0.016$ respectively. The three month seasonal mean shows a correlation ($R^2 = 0.35$) for winter (DJF) and no correlation for summer months JJA ($R^2 = 0.004$). Teranes and McKenzie (2001) showed that isotope data in Bern and NAO index are in good agreement for the period 1972–1995. We observed indeed a high correlation between three months NAO index versus winter (DJF) $\delta^{18}O_p$ in Basel for the period 1986–1995 ($R^2 = 0.75$) in agreement with Baldini et al. (2008), whereas a lower correlation ($R^2 = 0.28$) is observed for the period 1995–2012. Further investigations would be necessary on Milandre speleothem isotope records to see if such an influence is also detected.

In summary, for NW Switzerland $\delta^{18}O_p$ is mainly controlled by the temperature at the study site (Schürch et al., 2003; this study).

Correlation maps between $\delta^{18}O_p$ and temperature (Fig. 3c) show a significant correlation for Western Central Europe and isotopes are related to temperature both on a short (2 years) and on a long interval (25 years). Together with the temperature effect, a discernible influence of large scale atmospheric effects (NAO) on $\delta^{18}O_p$ is expected (Teranes and McKenzie, 2001) which will mainly have an influence on winter moisture source conditions. A good correlation is observed between the NAO index and the DJF months at the study site but no correlation is seen on a daily precipitation basis. Finally, for the precipitation amount, no significant correlation is observed either at the study site location on a two year time scale or when comparing with the 25 year CEP Basel station record (Fig. 3d).

4.7. Local meteoric water lines

4.7.1. Local meteoric water line from $\delta^{18}O$ and δD

The local meteoric water line (LMWL) has been determined for NW Switzerland using the relationship between δD and $\delta^{18}O$ on daily precipitation samples collected between March 2012 and March 2014. The least square regression equation corresponds to $\delta D = 7.92\,(\pm 0.07) \times \delta^{18}O + 7.26\,(\pm 0.70)\,(R^2 = 0.98)$ which is close to the Global Meteoric Water Line (GMWL, $\delta D = 8 \times \delta^{18}O + 10$). In addition, winter ($\delta D = 8.21 \times \delta^{18}O + 10.62$, $R^2 = 0.98$) and summer ($\delta D = 7.62 \times \delta^{18}O + 4.74$, $R^2 = 0.95$) meteoric water lines are shown in Fig. 8a. Lower d-excess (4.74‰) and a slightly lower slope indicate evaporation probably mainly occurring in the open gauge used for collection. Fig. 8a summarises all precipitation isotope values produced in this study, whereas Fig. 8b shows cave and fluid inclusion waters along with the LMWL and GMWL. Cave waters are close to the LMWL and shifted following the LMWL to more positive values. Eventually, the LMWL will be used for future paleotemperature calculations from speleothem fluid inclusions (e.g. Kim and ONeil, 1997; Tremaine et al., 2011).

4.7.2. Local meteoric water line from $\delta^{18}O$ and $\delta^{17}O$

The relationship between $\delta^{17}O$ and $\delta^{18}O$ in meteoric waters from NW Switzerland is presented in Fig. 9 together with the relationship for drip waters and specific monitored site location. The slope that relates the local liquid water and vapour at equilibrium (LMWL for oxygen) is 0.527 similar to the GMWL for oxygen defined by Luz and Barkan (2010) of 0.528. In upstream cave waters slight variations are observed with a lower slope of 0.518 measured on 40 samples only, but integrated over two years. The cave slope corresponds to the values of terrestrial biospheric exchange (respiration) of Luz and Barkan (2005) with a slope of 0.5179 ± 0.0006 and leaf transpiration slope of Landais et al. (2007).

4.8. Residence time and isotope shift between surface and cave

The transfer time for water infiltrating the soil and epikarst above the cave and its corresponding exit from the M6 soda straw inside the cave was assessed. The estimation of water residence time (τ) in the aquifer was based on isotope delay as well as the amplitude dampening between precipitation and drip water. First series of measurements performed with Picarro L1102-i and performed after each field sampling at M6 and Fi-2 drip sites yield a minimal time shift of around 8–10 months and an amplitude of 0.4‰, i.e. 25 times lower than for precipitation (Fig. 10). Noteworthy is that the re-measurements using a Picarro L2140-i made one to three years after the water sampling show hardly any seasonality at M6 but still show some at Fi-2 drip site, maybe due to sample alteration during storage. Without a weighted mean, this smoothing would be far too high keeping the observed residence time. Thus, a weighting is required. This is in line with the seasonal behaviour of drip rates, low during summer and high during winter.
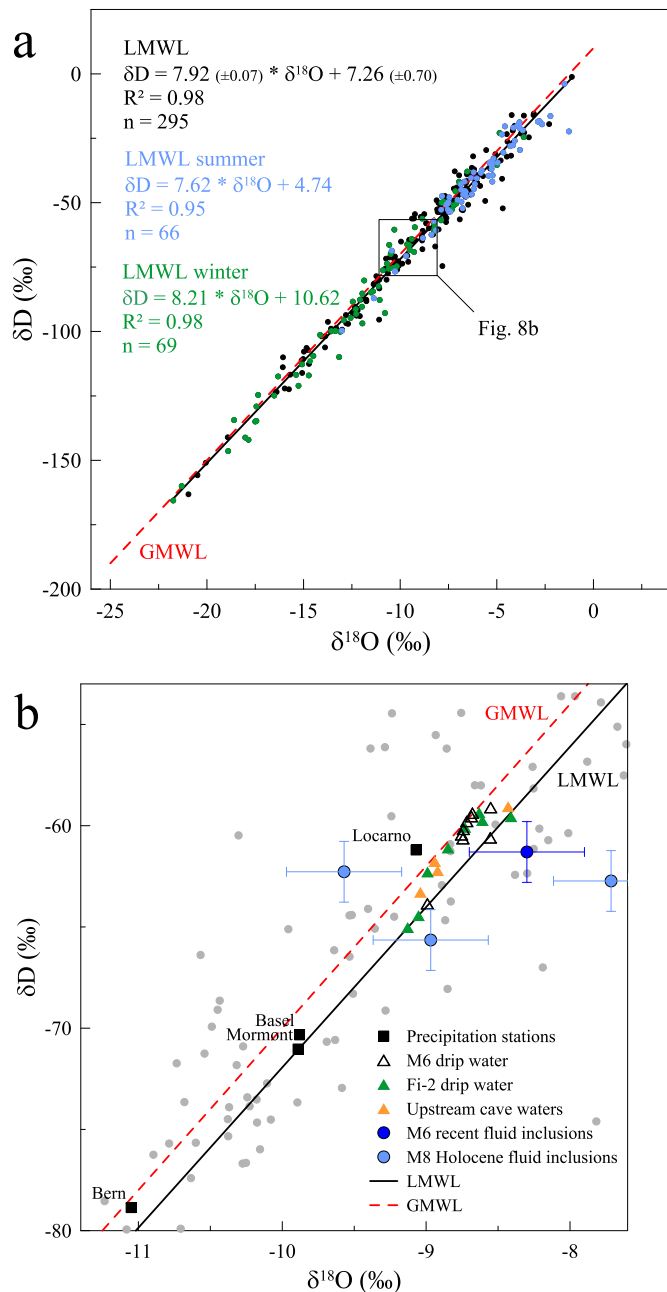
Fig. 8. (a) Local meteoric water line from δD and $\delta^{18}O$ in precipitation for Mormont station. Winter (DJF, green dots) and summer (JJA, blue dots) meteoric water line and associated regression based on two seasons. (b) Zoom that summarises mean isotope values from this study plotted together with the local meteoric water line and the global meteoric water line (dashed). Grey dots represent daily precipitation values. (For interpretation of the references to colour in this figure legend, the reader is referred to the web version of this article.)
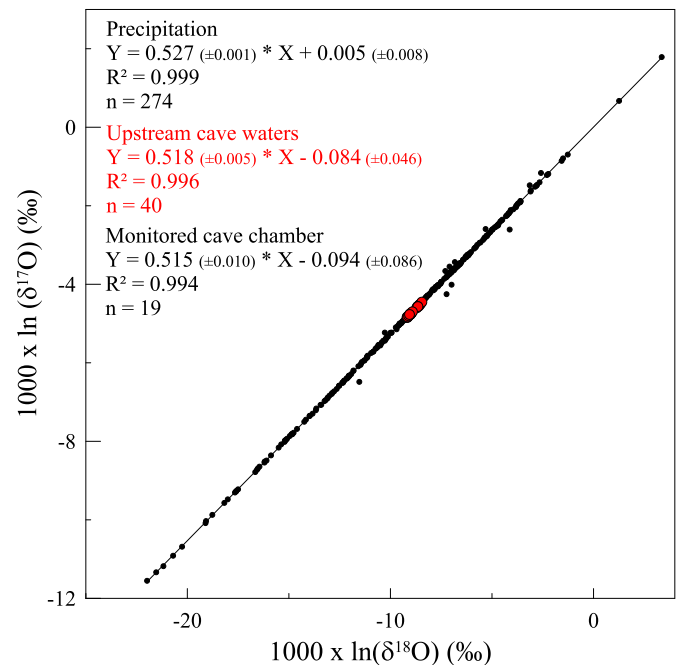

Fig. 9. Local meteoric water line from $\delta^{17}O$ and $\delta^{18}O$ in precipitation (black dots) for Mormont station and for drip waters (large red dots). (For interpretation of the references to colour in this figure legend, the reader is referred to the web version of this article.)
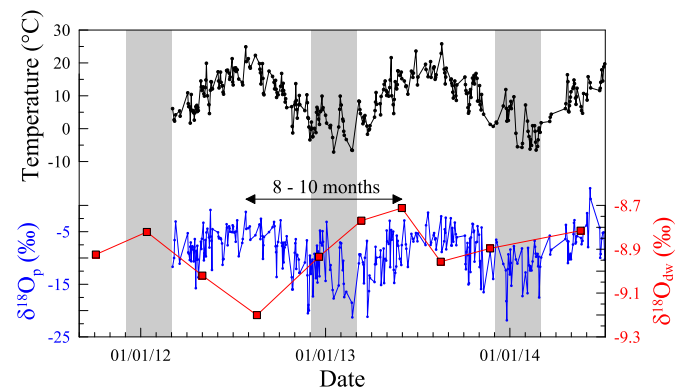

Fig. 10. Relationship between $\delta^{18}O$ in precipitation at Mormont station and in M6 drip water. Temperatures at Fahy station are shown in the upper panel. Winter seasons (DJF) are highlighted in grey.

During summer, water will preferentially be used by vegetation or evaporated and only partly be stored in the reservoir, whereas during the winter precipitation is infiltrating into the aquifer exhibiting more negative isotope values. Thus, a clear asymmetry between winter and summer infiltration occurs (Fig. 1) and leads to more negative values that are in contrast with the measurements that requires further explanation, given in the next paragraph. Finally, a mixing of 8−10 months mixing associated with a monthly weighted drip rate is able to explain the amplitude smoothing and the temporal shift of the signal in cave drip water. To further investigate the residence time issue, tritium isotope measurements on the collected cave water samples could be performed (Kluge et al., 2010). However, precision may not be sufficient to solve the issue completely.

After crossing the aquifer, the smoothed $\delta^{18}O_{dw}$ isotope signal exiting in the cave is 1‰ (respectively 10‰ for δD_{dw}) more positive than in precipitation. This enrichment cannot be explained by a trend in isotope variation in precipitation alone, as precipitation values are stable in the range of 0.5‰ within the monitoring time interval. Instead, the enrichment observed in both δD_{dw} and $\delta^{18}O_{dw}$ isotopes may be due to recycled condensed water inside the aquifer (Luo et al., 2013), but in Milandre cave, evapotranspiration occurring at the surface prior to infiltration is probably sufficient to explain this enrichment. Evaporation processes at the surface will tend to evaporate preferentially lighter water molecules meaning that the heavier ones will infiltrate the aquifer, which leads to isotope enrichment. Already 10−20% evaporated water accounts

for the observed isotopic enhancement. This is consistent with a slope change between precipitation and cave water for oxygen isotopes (Fig. 9).

Epikarst storage in Milandre karst aquifer (Perrin et al., 2003b) and infiltration of meteoric waters for the corresponding catchment area (Perrin et al., 2003a) have been carefully described and can be summarised as follows: soil and epikarst act as an important groundwater storage of the karst system and/or water circulates slowly in the unsaturated zone. The transit time is long enough for the water to reach equilibrium with calcite and water chemistry is mainly driven by the mixing of water derived from different infiltration zones in the epikarst (Williams, 2008). Moreover, Perrin et al. (2003b) observed stable $\delta^{18}O$ values of 9.15 ± 0.21‰ between June 1999 and July 2000 for waters coming from 15 cave sites. Isotope values showed low variability in time and location, so he defines $\delta^{18}O$ as a conservative tracer for precipitation flowing out of the cave at Saivu spring (Fig. 1). In this study, $\delta^{18}O$ "upstream" cave waters are on average ~0.3‰ more positive ($-8.83 ± 0.27$‰). This enrichment agrees with the trend observed in precipitation from Basel and Bern CEP stations of 0.02‰/year. Indeed, multiplying the trend by 14 years leads to an enrichment of 0.28‰ in precipitation close to the observations made in Milandre cave.

5. Conclusions

Oxygen ($\delta^{17}O$, $\delta^{18}O$) and hydrogen (δD) isotope evolution recorded during a two year monitoring period in precipitation, drip water and speleothem fluid inclusions for Milandre cave (NW Switzerland) is presented. Seasonal variations are visible in precipitation with more enriched values in summer and depleted in winter. Water isotopes in NW Switzerland precipitation are mainly controlled by air temperature (73%) on a monthly basis. A low correlation of 17% is observed with local relative humidity, but no correlation is observed with the amount of precipitation. Preliminary observations suggest that an influence of large scale atmospheric effects such as NAO on $\delta^{18}O_p$ occurs mainly during winter months.

Isotope values are enriched by around 10‰ for δD and 1‰ for $\delta^{18}O$ in drip water compared to weighted precipitation values which can be explained by evaporative processes at the surface prior to infiltration in the aquifer. Nevertheless, the isotope signal is smoothed to a high degree due to mixing in the soil and epikarst and of residence time of around 8–10 months in the aquifer above the cave. The climatic signal is shifted towards more positive values in drip water and hardly shows any seasonality (annual amplitude of 0.4‰) smoothed by a factor of ~25 compared to precipitation (annual amplitude of 10‰). Analyses of M6 and M8 stalagmite fluid inclusions coming from the monitored cave chamber showed that the mean annual drip water signal is preserved after its enclosure in speleothem calcite for recent samples allowing speleothem based paleoclimate reconstruction in Milandre cave. The cave located at the border between France and Switzerland presents climate conditions representative for Western Central Europe.

After a few adaptations of our measuring line, we successfully performed the first $\delta^{17}O$ measurements of fluid inclusion water together with δD and $\delta^{18}O$ on a single speleothem sample. This analytical advance may allow expanding the speleothem based paleoclimate reconstruction possibilities to the $^{17}O_{excess}$ parameter as it has already been done for ice cores (Winkler et al., 2012).

In this study, we showed for the first time that the $\delta^{17}O$ signal is preserved between precipitation and cave water with the two year monitoring. The parameter $^{17}O_{excess}$ shows equivalent averaged values of 18 per meg in both precipitation and drip water, whereas we have shown that $^{17}O_{excess}$ results measured in fluid inclusions produce values in the same range as surface precipitation.

Extended instrument calibration, as well as the use of several replicates, may help obtain more robust values. These results are promising and retrieving past information about the moisture source based on speleothem fluid inclusions is potentially achievable but more has to be learned. Analytical precision in $\delta^{18}O_{fi}$ and $\delta^{17}O_{fi}$ measurements is the key to detecting precise variations in $^{17}O_{excess}$.

Investigations of geochemical parameters, the understanding of processes as well as cave accessibility and speleothem richness and preservation allow us to define Milandre cave as a good candidate for paleoclimate reconstructions.

Appendix A. Supplementary data

Supplementary data related to this article can be found at http://dx.doi.org/10.1016/j.quascirev.2015.08.030.

References

Affolter, S., Fleitmann, D., Leuenberger, M., 2014. New online method for water isotope analysis of speleothem fluid inclusions using laser absorption spectroscopy (WS-CRDS). Clim. Past. 10, 1291–1304.

Angert, A., Cappa, C.D., DePaolo, D.J., 2004. Kinetic O-17 effects in the hydrologic cycle: indirect evidence and implications. Geochim. Cosmochim. Acta 68, 3487–3495.

Araguas-Araguas, L., Froehlich, K., Rozanski, K., 2000. Deuterium and oxygen-18 isotope composition of precipitation and atmospheric moisture. Hydrol. Process 14, 1341–1355.

Arienzo, M.M., Swart, P.K., Vonhof, H.B., 2013. Measurement of $\delta^{18}O$ and δ^2H values of fluid inclusion water in speleothems using cavity ring-down spectroscopy compared with isotope ratio mass spectrometry. Rapid Commun. Mass Sp. 27, 2616–2624.

Baldini, L.M., McDermott, F., Foley, A.M., Baldini, J.U.L., 2008. Spatial variability in the European winter precipitation delta(18)O-NAO relationship: Implications for reconstructing NAO-mode climate variability in the Holocene. Geophys Res. Lett. 35.

Barkan, E., Luz, B., 2005. High precision measurements of O-17/O-16 and O-18/O-16 ratios in H_2O. Rapid Commun. Mass Sp. 19, 3737–3742.

Barkan, E., Luz, B., 2007. Diffusivity fractionations of $(H_2O)-O_{16}/(H_2O)-O_{17}$ and $(H_2O)-O_{16}/(H_2O)-O_{18}$ in air and their implications for isotope hydrology. Rapid Commun. Mass Sp. 21, 2999–3005.

Blyth, A.J., Smith, C.I., Drysdale, R.N., 2013. A new perspective on the delta C-13 signal preserved in speleothems using LC-IRMS analysis of bulk organic matter and compound specific stable isotope analysis. Quat. Sci. Rev. 75, 143–149.

Burns, S.J., Fleitmann, D., Matter, A., Neff, U., Mangini, A., 2001. Speleothem evidence from Oman for continental pluvial events during interglacial periods. Geology 29, 623–626.

Cheng, H., Edwards, R.L., Broecker, W.S., Denton, G.H., Kong, X.G., Wang, Y.J., Zhang, R., Wang, X.F., 2009. Ice age terminations. Science 326, 248–252.

Cheng, H., Edwards, R.L., Shen, C.C., Polyak, V.J., Asmerom, Y., Woodhead, J., Hellstrom, J., Wang, Y.J., Kong, X.G., Spötl, C., Wang, X.F., Alexander, E.C., 2013. Improvements in Th-230 dating, Th-230 and U-234 half-life values, and U-Th isotopic measurements by multi-collector inductively coupled plasma mass spectrometry. Earth Planet S. C. Lett. 371, 82–91.

Collister, C., Mattey, D., 2008. Controls on water drop volume at speleothem drip sites: an experimental study. J. Hydrology 358, 259–267.

Craig, H., 1965. The measurement of oxygen isotope paleotemperatures. Stable isotopes Oceanogr. Stud. Palaeotemperatures 23, 166–182.

Cruz, F.W., Karmann, I., Viana, O., Burns, S.J., Ferrari, J.A., Vuille, M., Sial, A.N.,

Moreira, M.Z., 2005. Stable isotope study of cave percolation waters in sub-tropical Brazil: implications for paleoclimate inferences from speleothems. Chem. Geol. 220, 245–262.

Cuthbert, M.O., Baker, A., Jex, C.N., Graham, P.W., Treble, P.C., Andersen, M.S., Ian Acworth, R., 2014. Drip water isotopes in semi-arid karst: implications for speleothem paleoclimatology. Earth Planet S. C. Lett. 395, 194–204.

Dansgaard, W., 1964. Stable isotopes in precipitation. Tellus 16, 436–468.

Duan, F.C., Wu, J.Y., Wang, Y.J., Edwards, R.L., Cheng, H., Kong, X.G., Zhang, W.H., 2015. A 3000-yr annually laminated stalagmite record of the Last Glacial maximum from Hulu Cave, China. Quat. Res. 83, 360–369.

Dublyansky, Y.V., Spötl, C., 2009. Hydrogen and oxygen isotopes of water from inclusions in minerals: design of a new crushing system and on-line continuous-flow isotope ratio mass spectrometric analysis. Rapid Commun. Mass Sp. 23, 2605–2613.

Fleitmann, D., Burns, S.J., Neff, U., Mangini, A., Matter, A., 2003. Changing moisture sources over the last 330,000 years in Northern Oman from fluid-inclusion evidence in speleothems. Quat. Res. 60, 223–232.

Fleitmann, D., Burns, S.J., Neff, U., Mudelsee, M., Mangini, A., Matter, A., 2004. Palaeoclimatic interpretation of high-resolution oxygen isotope profiles derived from annually laminated speleothems from Southern Oman. Quat. Sci. Rev. 23, 935–945.

Fleitmann, D., Cheng, H., Badertscher, S., Edwards, R.L., Mudelsee, M., Gokturk, O.M., Fankhauser, A., Pickering, R., Raible, C.C., Matter, A., Kramers, J., Tuysuz, O., 2009. Timing and climatic impact of Greenland interstadials recorded in stalagmites from northern Turkey. Geophys. Res. Lett. 36.

Friedman, I., O'Neil, J.R., 1977. Compilation of stable isotope fractionation factors of geochemical interest. Paper 440-KK. In: Fleischer, M. (Ed.), Data of Geochemistry, sixth ed. U.S. Geol. Survey Prof, pp. 1–12.

Genty, D., Combourieu-Nebout, N., Peyron, O., Blamart, D., Wainer, K., Mansuri, F., Ghaleb, B., Isabello, L., Dormoy, I., von Grafenstein, U., Bonelli, S., Landais, A., Brauer, A., 2010. Isotopic characterization of rapid climatic events during OIS3 and OIS4 in Villars Cave stalagmites (SW-France) and correlation with Atlantic and Mediterranean pollen records. Quat. Sci. Rev. 29, 2799–2820.

Genty, D., Labuhn, I., Hoffmann, G., Danis, P.A., Mestre, O., Bourges, F., Wainer, K., Massault, M., Van Exter, S., Regnier, E., Orengo, P., Falourd, S., Minster, B., 2014. Rainfall and cave water isotopic relationships in two South-France sites. Geochim. Cosmochim. Acta 131, 323–343.

Gigon, R., Wenger, R., 1986. Inventaire Spéléologique de la Suisse. II. Canton du Jura. Commission Spéléologique de la Société helvétique des Sciences Naturelles, Porrentruy, Switzerland.

Griffiths, M.L., Drysdale, R.N., Vonhof, H.B., Gagan, M.K., Zhao, J.X., Ayliffe, L.K., Hantoro, W.S., Hellstrom, J.C., Cartwright, I., Frisia, S., Suwargadi, B.W., 2010. Younger Dryas-Holocene temperature and rainfall history of southern Indonesia from delta O-18 in speleothem calcite and fluid inclusions. Earth Planet S. C. Lett. 295, 30–36.

Guyard, H., Chapron, E., St-Onge, G., Labrie, J., 2013. Late-Holocene NAO and oceanic forcing on high-altitude proglacial sedimentation (Lake Bramant, Western French Alps). Holocene 23, 1163–1172.

Harris, I., Jones, P.D., Osborn, T.J., Lister, D.H., 2014. Updated high-resolution grids of monthly climatic observations – the CRU TS3.10 Dataset. Int. J. Climatol. 34, 623–642.

Häuselmann, A.D., 2013. Younger dryas and Holocene temperature variations recorded in stalagmites from Milandre cave, Switzerland. In: Isotopes of Carbon, Water, and Geotracers in Paleoclimate Research, 26–28 August 2013, Bern, Switzerland.

Henderson, G.M., 2006. Climate – caving in to new chronologies. Science 313, 620–622.

Hurrell, J., Van Loon, H., 1997. Decadal variations in climate associated with the North Atlantic oscillation. In: Diaz, H., Beniston, M., Bradley, R. (Eds.), Climatic Change at High Elevation Sites. Springer, Netherlands, pp. 69–94.

Jeannin, P.Y., 1996. PhD Thesis, CHYN, University of Neuchàtel, Switzerland.

Jouzel, J., Merlivat, L., 1984. Deuterium and O-18 in precipitation – modeling of the isotopic effects during snow formation. J. Geophys Res. Atmos. 89, 1749–1757.

Kennett, D.J., Breitenbach, S.F.M., Aquino, V.V., Asmerom, Y., Awe, J., Baldini, J.U.L., Bartlein, P., Culleton, B.J., Ebert, C., Jazwa, C., Macri, M.J., Marwan, N., Polyak, V., Prufer, K.M., Ridley, H.E., Sodemann, H., Winterhalder, B., Haug, G.H., 2012. Development and disintegration of Maya political systems in response to climate change. Science 338, 788–791.

Kim, S.T., O'Neil, J.R., 1997. Equilibrium and nonequilibrium oxygen isotope effects in synthetic carbonates. Geochim. Cosmochim. Acta 61, 3461–3475.

Kluge, T., Riechelmann, D.F.C., Wieser, M., Spötl, C., Sultenfuss, J., Schroder-Ritzrau, A., Niggemann, S., Aeschbach-Hertig, W., 2010. Dating cave drip water by tritium. J. Hydrol. 394, 396–406.

Krüger, Y., Marti, D., Staub, R.H., Fleitmann, D., Frenz, M., 2011. Liquid-vapour homogenisation of fluid inclusions in stalagmites: evaluation of a new thermometer for palaeoclimate research. Chem. Geol. 289, 39–47.

Lachniet, M.S., 2009. Climatic and environmental controls on speleothem oxygen-isotope values. Quat. Sci. Rev. 28, 412–432.

Landais, A., Barkan, E., Luz, B., 2008. Record of delta O-18 and O-17-excess in ice from Vostok Antarctica during the last 150,000 years. Geophys Res. Lett. 35.

Landais, A., Barkan, E., Yakir, D., Luz, B., 2006. The triple isotopic composition of oxygen in leaf water. Geochim. Cosmochim. Acta 70, 4105–4115.

Landais, A., Ekaykin, A., Barkan, E., Winkler, R., Luz, B., 2012a. Seasonal variations of O-17-excess and d-excess in snow precipitation at Vostok station, East Antarctica. J. Glaciol. 58, 725–733.

Landais, A., Risi, C., Bony, S., Vimeux, F., Descroix, L., Falourd, S., Bouygues, A., 2010. Combined measurements of O-17(excess) and d-excess in African monsoon precipitation: implications for evaluating convective parameterizations. Earth Planet S. C. Lett. 298, 104–112.

Landais, A., Steen-Larsen, H.C., Guillevic, M., Masson-Delmotte, V., Vinther, B., Winkler, R., 2012b. Triple isotopic composition of oxygen in surface snow and water vapor at NEEM (Greenland). Geochim. Cosmochim. Acta 77, 304–316.

Landais, A., Yakir, D., Barkan, E., Luz, B., 2007. The triple isotopic composition of oxygen in leaf water and its implications for quantifying biosphere productivity. In: Todd, E.D., Rolf, T.W.S. (Eds.), Terrestrial Ecology. Elsevier, pp. 111–125.

Li, S., Levin, N.E., Chesson, L.A., 2015. Continental scale variation in 17O-excess of meteoric waters in the United States. Geochim. Cosmochim. Acta 164, 110–126.

Luetscher, M., Boch, R., Sodemann, H., Spötl, C., Cheng, H., Edwards, R.L., Frisia, S., Hof, F., Muller, W., 2015. North Atlantic storm track changes during the Last Glacial maximum recorded by Alpine speleothems. Nat. Commun. 6.

Luetscher, M., Jeannin, P.Y., 2004. Temperature distribution in karst systems: the role of air and water fluxes. Terra Nova 16, 344–350.

Luo, W.J., Wang, S.J., Xie, X.N., 2013. A comparative study on the stable isotopes from precipitation to speleothem in four caves of Guizhou, China. Chem. Erde-Geochem 73, 205–215.

Luz, B., Barkan, E., 2005. The isotopic ratios 17O/16O and 18O/16O in molecular oxygen and their significance in biogeochemistry. Geochim. Cosmochim. Acta 69, 1099–1110.

Luz, B., Barkan, E., 2010. Variations of O-17/O-16 and O-18/O-16 in meteoric waters. Geochim. Cosmochim. Acta 74, 6276–6286.

Mangini, A., Spötl, C., Verdes, P., 2005. Reconstruction of temperature in the Central Alps during the past 2000 yr from a delta O-18 stalagmite record. Earth Planet S. C. Lett. 235, 741–751.

McDermott, F., Schwarcz, H., Rower, P.J., 2006. Isotopes in speleothems. In: Leng, M.J. (Ed.), Isotopes in Paleoenvironmental Research. Springer, The Netherlands.

Meckler, A.N., Affolter, S., Dublyanski, Y.V., Krüger, Y., Vogel, N., Bernasconi, S.M., Frenz, M., Kipfer, R., Leuenberger, M., Spötl, C., Carolin, S., Cobb, K.M., Moerman, J., Adkins, J.F., Fleitmann, D., 2015. Glacial-interglacial temperature change in the tropical West Pacific: a comparison of stalagmite-based paleothermometers. Quat. Sci. Rev. http://dx.doi.org/10.1016/j.quascirev.2015.06.015.

Meckler, A.N., Clarkson, M.O., Cobb, K.M., Sodemann, H., Adkins, J.F., 2012. Interglacial hydroclimate in the tropical west Pacific through the late pleistocene. Science 336, 1301–1304.

Meckler, A.N., Ziegler, M., Millan, M.I., Breitenbach, S.F.M., Bernasconi, S.M., 2014. Long-term performance of the Kiel carbonate device with a new correction scheme for clumped isotope measurements. Rapid Commun. Mass Sp. 28, 1705–1715.

Moerman, J.L., Cobb, K.M., Kollmeyer, R., Clark, B., Tuen, A.A., 2010. Climatic influences on daily rainwater delta O-18 and delta D timeseries in Northern Borneo. Geochim. Cosmochim. Acta 74. A716–A716.

Moreno, A., Sancho, C., Bartolome, M., Oliva-Urcia, B., Delgado-Huertas, A., Estrela, M.J., Corell, D., Lopez-Moreno, J.I., Cacho, I., 2014. Climate controls on rainfall isotopes and their effects on cave drip water and speleothem growth: the case of Molinos cave (Teruel, NE Spain). Clim. Dynam. 43, 221–241.

Niggemann, S., Mangini, A., Richter, D.K., Wurth, G., 2003. A paleoclimate record of the last 17,600 years in stalagmites from the B7 cave, Sauerland, Germany. Quat. Sci. Rev. 22, 555–567.

Perrin, J., 2003. A Conceptual Model of Flow and Transport in a Karst Aquifer Based on Spatial and Temporal Variations of Natural Tracers. PhD Thesis. CHYN, University of Neuchàtel, Switzerland.

Perrin, J., Jeannin, P.Y., Cornaton, F., 2007. The role of tributary mixing in chemical variations at a karst spring, Milandre, Switzerland. J. Hydrol. 332, 158–173.

Perrin, J., Jeannin, P.Y., Zwahlen, F., 2003a. Implications of the spatial variability of infiltration-water chemistry for the investigation of a karst aquifer: a field study at Milandre test site, Swiss Jura. Hydrogeol. J. 11, 673–686.

Perrin, J., Jeannin, P.Y., Zwahlen, F., 2003b. Epikarst storage in a karst aquifer: a conceptual model based on isotopic data, Milandre test site. Switz. J. Hydrol. 279, 106–124.

Pfahl, S., Sodemann, H., 2014. What controls deuterium excess in global precipitation? Clim. Past. 10, 771–781.

Riechelmann, D.F.C., Schroder-Ritzrau, A., Scholz, D., Fohlmeister, J., Spötl, C., Richter, D.K., Mangini, A., 2011. Monitoring Bunker Cave (NW Germany): a prerequisite to interpret geochemical proxy data of speleothems from this site. J. Hydrol. 409, 682–695.

Rolland, C., 2003. Spatial and seasonal variations of air temperature lapse rates in Alpine regions. J. Clim. 16, 1032–1046.

Rozanski, K., Araguasaraguas, L., Gonfiantini, R., 1992. Relation between long-term trends of O-18 isotope composition of precipitation and climate. Science 258, 981–985.

Rudzka, D., McDermott, F., Baldini, L.M., Fleitmann, D., Moreno, A., Stoll, H., 2011. The coupled delta C-13-radiocarbon systematics of three Late Glacial/early Holocene speleothems; insights into soil and cave processes at climatic transitions. Geochim. Cosmochim. Acta 75, 4321–4339.

Schmassmann, S., 2010. Speleothem-based Climate and Environmental Reconstruction: a Pilot Study in the Swiss Jura Mountains. Master Thesis. Geological Institute, University of Bern, Switzerland.

Schoenemann, S.W., Schauer, A.J., Steig, E.J., 2013. Measurement of SLAP2 and GISP 17O and proposed VSMOW-SLAP normalization for 17O and 17Oexcess. Rapid Commun. Mass Sp. 27, 582–590.

Schoenemann, S.W., Steig, E.J., Ding, Q.H., Markle, B.R., Schauer, A.J., 2014. Triple water-isotopologue record from WAIS Divide, Antarctica: controls on glacial-interglacial changes in O-17(excess) of precipitation. J. Geophys. Res. Atmos. 119, 8741—8763.

Schotterer, U., Stichler, W., Graf, W., Buerki, H.-U., Gourcy, L., Ginot, P., Huber, T., 2002. Stable Isotopes in Alpine Ice Cores: Do they Record Climate Variability?.

Schotterer, U., Stocker, T., Bürki, H., Hunziker, J., Kozel, R., Grasso, D.A., Tripet, J.P., 2000. Das Schweizer Isotopen-Messnetz. Trends 1992—1999. In: Gas, Wasser, Abwasser, pp. 733—741.

Schürch, M., Kozel, R., Schotterer, U., Tripet, J.P., 2003. Observation of isotopes in the water cycle — the Swiss National Network (NISOT). Environ. Geol. 45, 1—11.

Schwarcz, H.P., Harmon, R.S., Thompson, P., Ford, D.C., 1976. Stable isotope studies of fluid inclusions in speleothems and their paleoclimatic significance. Geochim. Cosmochim. Acta 40, 657—665.

Shakun, J.D., Burns, S.J., Fleitmann, D., Kramers, J., Matter, A., Al-Subary, A., 2007. A high-resolution, absolute-dated deglacial speleothem record of Indian Ocean climate from Socotra Island, Yemen. Earth Planet S. C. Lett. 259, 442—456.

Shen, C.C., Lin, K., Duan, W.H., Jiang, X.Y., Partin, J.W., Edwards, R.L., Cheng, H., Tan, M., 2013. Testing the annual nature of speleothem banding. Sci. Rep-Uk 3.

Singh, R., Kishtawal, C.M., Joshi, P.C., 2005. Estimation of monthly mean air-sea temperature difference from satellite observations using genetic algorithm. Geophys Res. Lett. 32.

Sodemann, H., Zubler, E., 2010. Seasonal and inter-annual variability of the moisture sources for Alpine precipitation during 1995—2002. Int. J. Climatol. 30, 947—961.

Steen-Larsen, H.C., Masson-Delmotte, V., Hirabayashi, M., Winkler, R., Satow, K., Prie, F., Bayou, N., Brun, E., Cuffey, K.M., Dahl-Jensen, D., Dumont, M., Guillevic, M., Kipfstuhl, S., Landais, A., Popp, T., Risi, C., Steffen, K., Stenni, B., Sveinbjornsdottir, A.E., 2014. What controls the isotopic composition of Greenland surface snow? Clim. Past. 10, 377—392.

Steig, E.J., Gkinis, V., Schauer, A.J., Schoenemann, S.W., Samek, K., Hoffnagle, J., Dennis, K.J., Tan, S.M., 2014. Calibrated high-precision O-17-excess measurements using cavity ring-down spectroscopy with laser-current-tuned cavity resonance. Atmos. Meas. Tech. 7, 2421—2435.

Teranes, J.L., McKenzie, J.A., 2001. Lacustrine oxygen isotope record of 20(th)-century climate change in central Europe: evaluation of climatic controls on oxygen isotopes in precipitation. J. Paleolimnol. 26, 131—146.

Tremaine, D.M., Froelich, P.N., Wang, Y., 2011. Speleothem calcite farmed in situ: modern calibration of delta O-18 and delta C-13 paleoclimate proxies in a continuously-monitored natural cave system. Geochim. Cosmochim. Acta 75, 4929—4950.

Uemura, R., Barkan, E., Abe, O., Luz, B., 2010. Triple isotope composition of oxygen in atmospheric water vapor. Geophys. Res. Lett. 37.

Uemura, R., Matsui, Y., Yoshimura, K., Motoyama, H., Yoshida, N., 2008. Evidence of deuterium excess in water vapor as an indicator of ocean surface conditions. J. Geophys. Res. Atmos. 113.

Vaks, A., Gutareva, O.S., Breitenbach, S.F.M., Avirmed, E., Mason, A.J., Thomas, A.L., Osinzev, A.V., Kononov, A.M., Henderson, G.M., 2013. Speleothems Reveal 500,000-Year history of Siberian permafrost. Science 340, 183—186.

van Breukelen, M.R., Vonhof, H.B., Hellstrom, J.C., Wester, W.C.G., Kroon, D., 2008. Fossil dripwater in stalagmites reveals Holocene temperature and rainfall variation in Amazonia. Earth Planet S. C. Lett. 275, 54—60.

van Rampelbergh, M., Verheyden, S., Allan, M., Quinif, Y., Keppens, E., Claeys, P., 2014. Monitoring of a fast-growing speleothem site from the Han-sur-Lesse cave, Belgium, indicates equilibrium deposition of the seasonal delta O-18 and delta C-13 signals in the calcite. Clim. Past. 10, 1871—1885.

Vogel, N., Brennwald, M.S., Fleitmann, D., Wieler, R., Maden, C., Susli, A., Kipfer, R., 2013. A combined vacuum crushing and sieving (CVCS) system designed to determine noble gas paleotemperatures from stalagmite samples. Geochem Geophys. Geosys. 14, 2432—2444.

Williams, P.W., 2008. The role of the epikarst in karst and cave hydrogeology: a review. Int. J. Speleol. 37, 1—10.

Winkler, R., Landais, A., Sodemann, H., Dumbgen, L., Prie, F., Masson-Delmotte, V., Stenni, B., Jouzel, J., 2012. Deglaciation records of O-17-excess in East Antarctica: reliable reconstruction of oceanic normalized relative humidity from coastal sites. Clim. Past. 8, 1—16.

Winkler, R., Landais, A., Risi, C., Baroni, M., Ekaykin, A., Jouzel, J., Petit, J.R., Prie, F., Minster, B., Falourd, S., 2013. Interannual variation of water isotopologues at Vostok indicates a contribution from stratospheric water vapor. Proc. Natl. Acad. Sci. U.S.A 110, 17674—17679.